Adaptation to complex environments reveals pervasive trade-offs and genetic targets with pleiotropic effects

Alexandre Rêgo[1,2*], Dragan Stajic[2,3*], Carla Bautista[4,5], Sofia Rouot[6], Maria de la Paz Celorio-Mancera[7], Rike Stelkens[2]

[1] Department of Ecology and Genetics, Uppsala University, Uppsala 752 36, Sweden

[2] Department of Zoology, Stockholm University, Stockholm 114 19, Sweden

[3] Institute for Fish and Wildlife Health, University of Bern, Bern 3012, Switzerland

[4] Institut de Biologie Intégrative et des Systèmes (IBIS), Université Laval, Québec, QC, Canada

[5] Département de Biologie, Faculté des Sciences et de Génie, Université Laval, Québec, QC, Canada

[6] SciLifeLab, Department of Gene Technology, KTH Royal Institute of Technology, Stockholm 171 65, Sweden

[7] Department of Ecology, Environment, and Plant Science (DEEP), Stockholm University, Stockholm 106 91, Sweden

* Shared first-authorship

Corresponding Author: Alexandre Rêgo, denovorego@gmail.com

Abstract

Keywords: evolve and resequence; Saccharomyces cerevisiae; complex environments; phenotypic evolution; trade-offs; genomic evolution

Much of our knowledge on the dynamics of adaptation comes from experimental evolution studies that expose populations to a single selective pressure. However, populations in nature rarely adapt to a single stress at a time. Instead, various biotic and abiotic factors come together to produce complex selective environments. Here, we used experimental evolution to describe adaptive dynamics in the presence of simultaneous stressors, and to quantify the evolution of trade-offs between stressors in a complex environment. We adapted populations of the yeast *Saccharomyces cerevisiae* to a full-factorial combination of four stressors over the course of 15 serial transfers. Rapid fitness increases were accompanied by the accumulation of mutations in genes and pathways related to specific stressors. Trade-offs evolved rapidly, with the order and mode of trade-off evolution varying between environments due to the inherent physiological and genetic basis of resistance to each stressor. Compensatory evolution for maladaptation as a result of initial trade-offs was typically mediated by fine-tuning of genes associated with the initially adapted environmental component, rather than those associated with the maladapted trait. As environmental complexity increased, mutations had increasingly broader effects across multiple biological processes. Although shared mutations at the individual SNP level were rare, recurrent mutations affecting the same genes and putative biological processes were abundant across environmental complexity. Our results suggest that adaptation in complex environments follows genetic trajectories shaped by pleiotropy and trade-offs, but these trajectories may impose lasting constraints on future adaptation.

Introduction

Natural habitats are rich with ecological complexity, resulting in many co-occurring sources of selection through biotic and abiotic factors (Orsini, Spanier, and DE Meester 2012). The dimensionality of concurrent selective pressures may even increase for populations in the Anthropocene, due to additional effects of pollution, urbanization, and climate change (Hendry, Gotanda, and Svensson 2017). Predicting the dynamics and

outcomes of adaptation to complex environments has been a long-standing goal with far-reaching implications, from conservation to the evolution of antimicrobial drug resistance (Hendry, Gotanda, and Svensson 2017; Sommer, Johansen, and Molin 2020). But measuring and describing adaptation in the wild is not trivial given logistical limitations to working with natural populations and the difficulty of assigning causes of selection in nature (Vandenkoornhuyse et al. 2010). Experimental evolution studies are now more often implementing temporally and spatially variable or multidimensional selection regimes as a bridge to investigate evolutionary dynamics in ecologically complex natural environments (Barrett, MacLean, and Bell 2005; Kram et al. 2017)(Hendry, Gotanda, and Svensson 2017; Sommer, Johansen, and Molin 2020)(Barrett, MacLean, and Bell 2005; Kram et al. 2017). Even so, few current studies integrate genomic sampling and time-series sampling to address the underlying genomic basis and dynamics of adaptation to complex environments.

Adaptation to complex environments is consistently marked by the existence of trade-offs (Garland, Downs, and Ives 2022). Theory predicts that a particular phenotype cannot be optimal for all selective pressures, and that most populations exist along a range of phenotypes that optimize fitness in multidimensional selection regimes (Shoval et al. 2012). Trade-offs for multiple traits, through resource limitation, antagonistic pleiotropy, genetic correlations, or epistasis are common (Roff and Fairbairn 2007; Garland, Downs, and Ives 2022). However, several experimental evolution studies show that populations can improve fitness in many dimensions simultaneously (Bennett and Lenski 2007; McGee et al. 2016; Bono et al. 2017). Empirical evidence of how trade-offs themselves evolve, and affect dynamics of adaptation over short time scales, is relatively scarce (Roff and Fairbairn 2007; Vincent et al. 2013; Bono et al. 2017).

Adaptation in complex environments is not only influenced by the prevalence of trade-offs. The dynamics of phenotypic evolution (i.e. the rate of fitness changes and trait trajectory) and genomic evolution (i.e. the rate of allele frequency change, and the number of adaptive mutations) can also be affected by the complexity of the environment. For example, when multiple stressors simultaneously increase the strength of selection, the

trajectory and rate of trait evolution can be altered (H. A. Orr 2005; Cisneros-Mayoral et al. 2022). Increased selection in more complex environments may also have demographic effects. Reduced population sizes can lead to reduced genetic diversity and mutational supply, as well as increased genetic drift (Ewens 1979). Furthermore, adaptation to multiple concurrent stressors may require distinct solutions that differ from those needed for individual stressors (Elena and Lenski 2003).

Many studies focus on adaptive outcomes and trade-offs, but only a few use time-series data to describe the dynamics of trade-off evolution itself (Huang et al. 2017; J. A. Orr et al. 2022). To understand how the dynamics and outcomes of adaptation differ between simple and complex environments, we used experimental evolution with the yeast *Saccharomyces cerevisiae.* Here we define simple environments as those manipulated along a single experimental dimension and complex environments as those manipulated along multiple dimensions, while acknowledging that even "simple" environments contain numerous factors that cannot be completely isolated or controlled. We evolved replicate lines in four single stressors and full-factorial combinations of the four stressors. We collected fitness and genomic time-series data to investigate the tempo and mode of adaptation at different biological scales, including trajectories in multidimensional adaptive space that populations explore when environmental stressors coincide. To test for the existence and genetic basis of trade-offs, we measured fitness and sequenced genomes of populations that had evolved in complex environments. We tested these populations in both the original complex selective media and in simpler media containing only one component at a time. Our goals were to determine (i) how the dynamics of adaptation depend on the complexity of the environment, (ii) how does the genetic basis of adaptation differ in complex environments (iii) to what extent trade-offs exist in complex environments, and (iv) how do these trade-offs evolve.

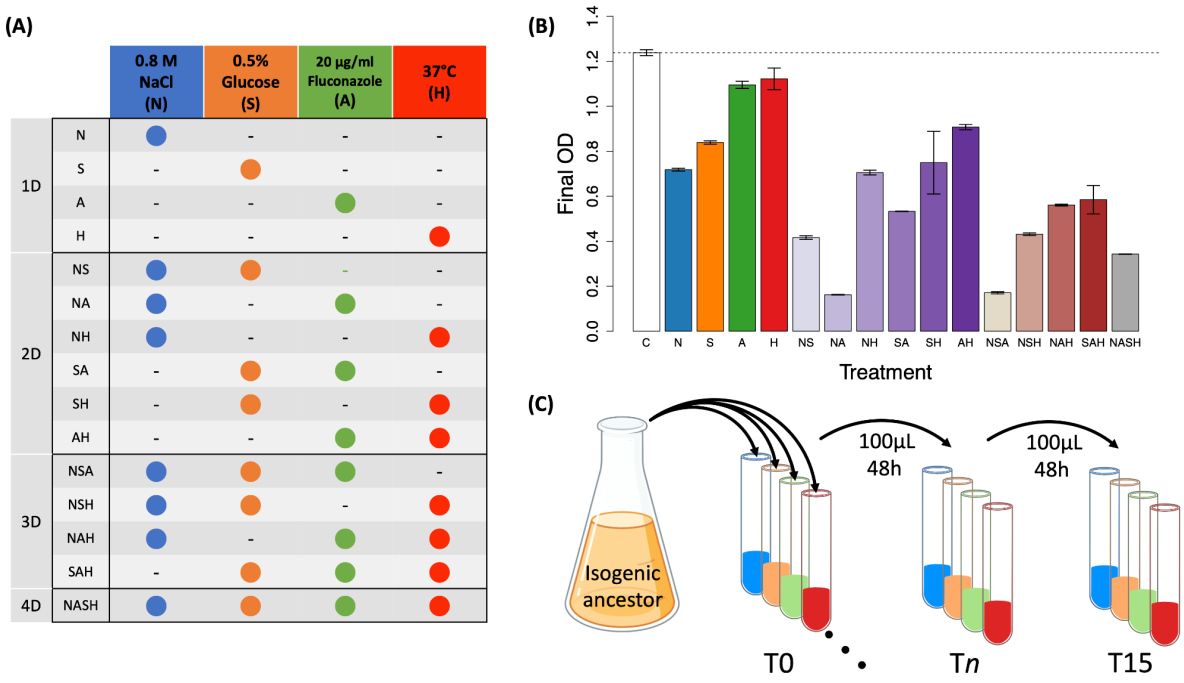

Figure 1. Experimental set-up and stressor effects for each environment. (A) Populations were evolved in every stressor and full-factorial combination of each. Colored dots represent the presence of a stressor. Abbreviations are given for each combination of stressors, as well as the 'dimensionality' (1D-4D) of the environmental complexity. (B) The stressor effect of each environment in the ancestor was measured as the difference in final OD after 24 hours in a selective environment relative to benign YPD medium. The mean estimate is given with standard error bars. (C) From an initially isogenic colony, four replicate populations of yeast were inoculated into each environment. Populations were then evolved through serial transfer every 48 hours where 2% (100µL) of the culture was transferred into fresh media, for a total of 15 transfers. Fitness measurements and whole genome, whole population sequencing were conducted at T7 and T15.

Results

Initially isogenic replicate lines of *S. cerevisiae* (four replicates per environment, 60 in total) were evolved in either single stressors (Figure 1A, 1D environments, designated with single-letter abbreviations) or the full-factorial combinations of multiple stressors (Figure 1A, 2D-4D environments, designated with multi-letter abbreviations). The four stressors used were high salinity (0.8M NaCl, designated "N"), the antifungal drug fluconazole (20µg/ml, "A"), starvation (0.5% glucose YPD, "S"), and high temperature (37°C, "H"). The selective pressure of each environment was quantified at the beginning of the experiment

as the difference in final optical density (OD600) after 24 hours relative to growth in a benign YPD environment ($\Delta OD = OD_{YPD} - OD_{Selected}$, Mean±SE) (Figure 1B, see Figure S1 for stressor effects based on growth rate). Of the 1D environments, the salt (ΔOD = -0.520±0.006) and starvation environments (ΔOD = -0.399±0.008) had the largest stressor effects, while antifungal (ΔOD = -0.143±0.159) and heat (ΔOD = -0.116±0.048) had more moderate effects (Figure 1B). Experimental evolution on each line was conducted for a total of 15 transfers with transfers occurring every 48 hours into fresh media (Figure 1C). Evolving lines were frozen at the midpoint of the experiment (T7) and the end (T15) for further genomic sequencing.

Rapid but plateauing adaptation to environmental stressors

To determine how much a replicate line had adapted, we measured the fitness of evolved lines relative to the fitness of the ancestral population in growth competition assays, designated as the selection coefficient (Gordo, Perfeito, and Sousa 2011). All lines showed evidence of adaptation at the midpoint of experimental evolution (T7), with few exceptions (all four replicates of SH, and NASH1) (Figure 2). The largest selection coefficient at the midpoint was observed in the antibiotic environment (S_{A2}=0.43). However, SA lines showed the highest selection coefficients on average ($\underline{S}_{SA}$=0.41, SE=0.007). By the midpoint of the experiment, the fitness of many populations had reached a fitness plateau after which fitness did not significantly increase again until the end of the experiment (paired *t*, p>0.05), with some exceptions (average of replicates for the N, NA, NH, NAH, SAH, and NSA lines). Despite many populations not differing significantly in fitness between T7 and T15, average gains in fitness between T7 and T15 did tend to increase as complexity levels increased ($\beta = 0.024$, $t(58) = 2.06$, $p = 0.044$), indicating that populations in more complex environments had not yet reached their local fitness optima.

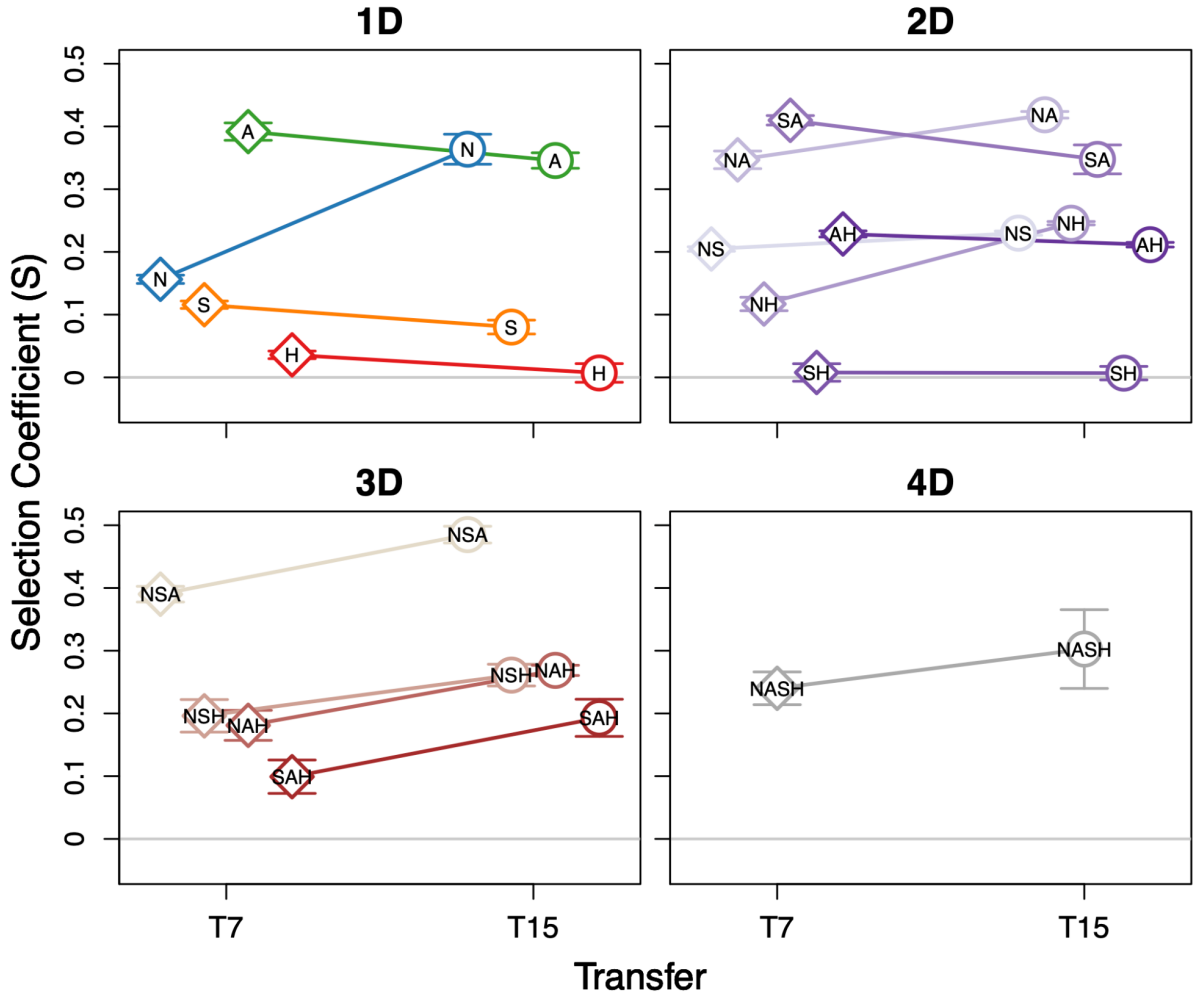

Figure 2. Selection coefficients at T7 and T15 for each environment, partitioned by environmental complexity level (1D–4D). Mean selection coefficients of the four replicates for each treatment are given as points while bars represent the standard deviations. T0 is excluded for visualization purposes, but would reside on the S=0 line.

Adaptation to complex environments reveals pervasive trade-offs

We tested for the existence of trade-offs during adaptation to the individual stressors (N, A, S, H) of the complex environments. For this, we compared the fitness of evolved lines adapted to complex environments to the fitness of single-stressor specialists in the respective single stress environment. Populations evolved in complex environments were unable to adapt to the same level of fitness as all single environment specialists in their respective environments, resulting in abundant trade-offs (Figure 3, Figure S2). For each of the four individual stressors, there were 7 complex environment combinations which

contained the stressor in our full-factorial design. The individual stressor with the highest prevalence of trade-offs (i.e. the proportion of complex environment-adapted lines which on average were unable to reach the fitness of single stressor specialists; t, $p<0.05$) was NaCl (6/7 complex-adapted lines), followed by Starvation (3/7), Heat (3/7), and Antifungal (1/7) (Figure S2, Figure S3).

To evaluate how well multi-stressor adapted lines (e.g., NAS lines) performed compared to single-stressor specialists (e.g., N, A, and S lines), we calculated their relative fitness (RF = $\frac{S_{complex}}{max\{S_{specialist}\}}$) in each respective environmental component. The evolution of trade-offs under heat stress showed a particularly strong initial fitness cost at T7 ($\underline{RF}$ = -1.60) which was later mitigated by T15 ($\underline{RF}$ = 0.05). Lines tested in other single stressors experienced less severe trade-offs, with $\underline{RF}$ gradually increasing: from 0.54 to 0.87 for antifungal, from 0.21 to 0.47 for salt, and from -0.04 to 0.43 for starvation (Figure S3). These results suggest that, when present, populations typically adapt to antifungal first, reaching a greater relative fitness than when adapting to any other stressors by T15. The adaptation of populations to antifungal seemed to incur negative trade-offs to heat stress, though these maladaptations were typically compensated for by T15 (Figure S3). Surprisingly though, some lines evolved in complex environments were able to exceed the fitness of the single-stressor specialists. This is especially true for NAH lines tested in antifungal medium and NS lines tested in starvation medium, where all replicates showed higher fitness than the specialists in the specialist's respective stressors (Figure S3, $p<0.05$).

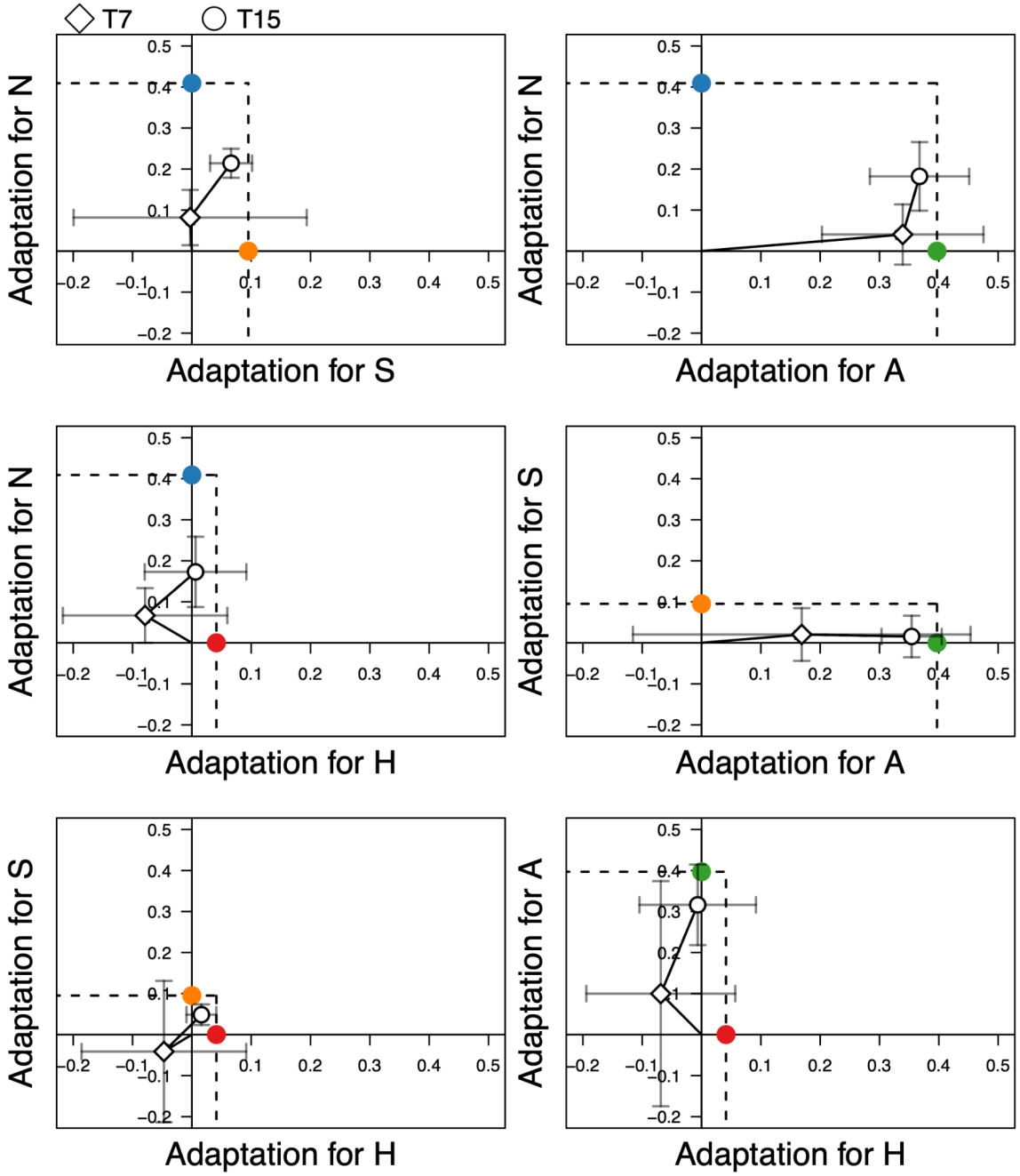

178

179 Figure 3. Trade-offs in adaptation to individual stressors within complex environments.
180 Each panel shows adaptation (relative fitness compared to ancestor) of populations
181 evolved in complex environments when tested in single-stressor conditions. For each
182 pairwise comparison, means (and ±1 sd bars) are shown for those complex environments
183 that contain both individual stressors as diamonds (at T7) and circles (at T15). Colored
184 dots represent the fitness of single-stressor specialists projected onto their respective axes.
185 The lower-left area of the black dotted lines represents the space in which populations
186 evolved in complex environments are expected to fall (i.e. less adapted in single-stress

environments than either 1D specialist).

Trade-off and cross-protective evolution to non-selected environments

To test for possible novel trade-off or cross-protective mechanisms between adaptation to different stresses, we tested the fitness of each population (all 1D–3D populations) in every respective environment not directly selected for during experimental evolution (e.g. N-evolved populations would be tested in A, S, and H environments individually, Figure 4). The strongest trade-offs across all evolved populations were observed in novel antifungal exposure, where the majority of evolved lines (6/7) showed a significantly reduced fitness in the presence of fluconazole at T7 (Figure 4, upper right panel; $\underline{S}_{A_T7}$= -0.24, SD = 0.19). While this sensitivity was reduced by the end of the experiment, it rarely led to a fitness advantage ($\underline{S}_{A_T15}$ = -0.16, SD = 0.16). In contrast, we often observed significant cross-protective responses in other non-selected environments by T15 (2/7 in S, 4/7 in N, and 5/7 in H) . This suggests the existence of cross-talk between stress response pathways to these different environmental stressors. We observed the largest cross-protection in the case of exposure to osmotic stress at T15 ($\underline{S}_{N_T15}$=0.049, SD = 0.09; Figure 4, upper left panel), where surprisingly even populations adapted to antifungal showed an increase in fitness, despite low fitness of N-evolved populations tested in the antifungal environment.

We tested whether the degree of environmental complexity a line evolved in (1D-3D) had a bearing on the degree of cross-protection to each novel environment (except NASH replicates as they were exposed to all stressors) with linear regression. By the end of experimental evolution, we found a negative association between fitness and complexity in the presence of salt and starvation ($p < 0.05$), whereas no association was found in either antifungal or heat (Figure S4).

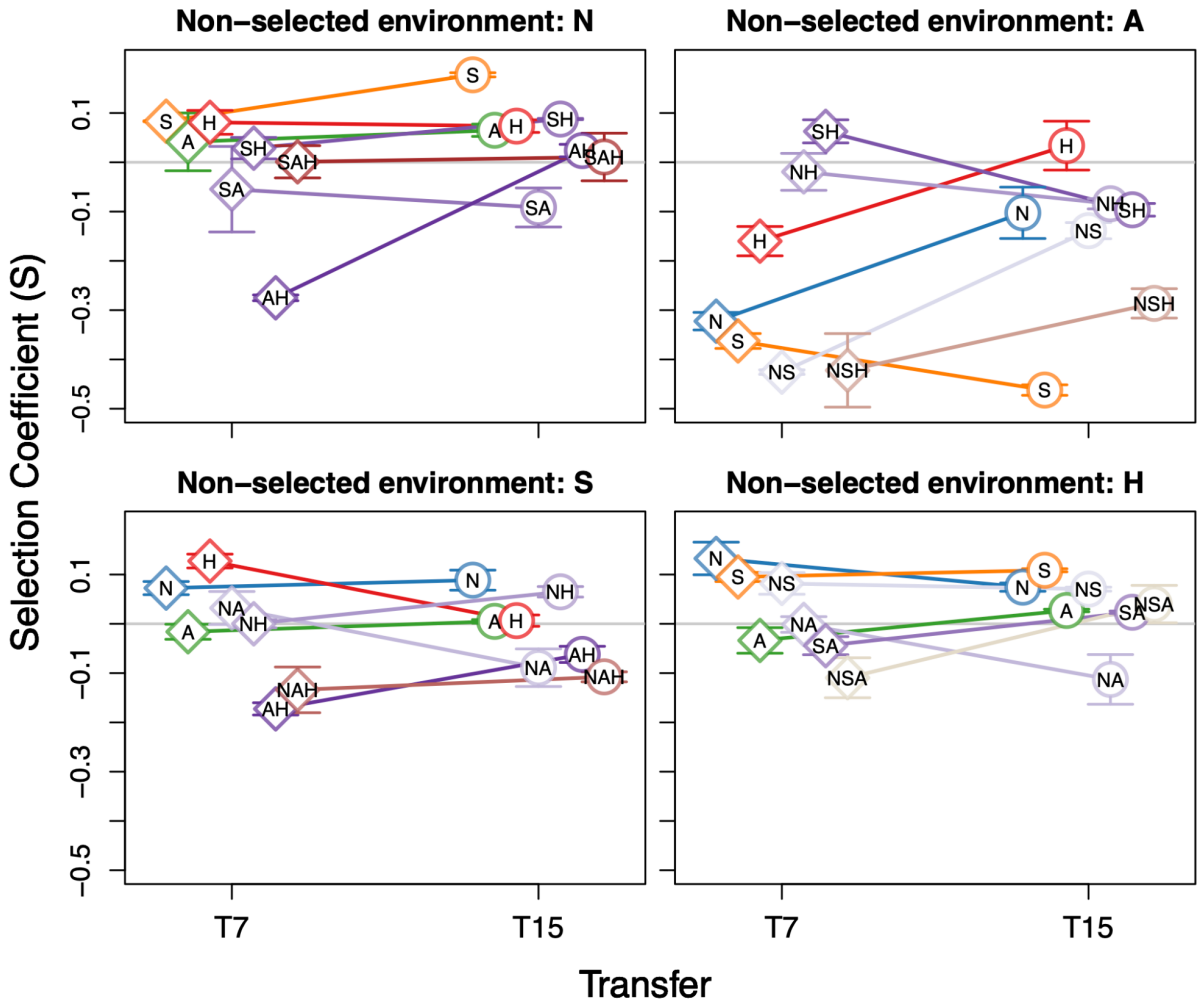

Figure 4. Patterns of trade-offs and cross-protection evolution in non-selected environments. Estimated selection coefficients are shown as diamonds or circles for T7 and T15, respectively, with bars as standard deviations. The grey line represents a selection coefficient of 0.

Fitness costs of adaptation

We tested for possible costs of adaptation to stressful environments by measuring the selection coefficient in the originally benign YPD environment for each evolved population at both time points (S_{YPD_Tn}). Across all treatments and lines, we observed an average decrease in fitness in YPD at T7 ($\underline{S}_{YPD_T7}$ = -0.022, SD= 0.13). However, this cost diminished (or was reversed) by T15 of the experimental evolution ($\underline{S}_{YPD_T15}$ = 0.013, SD = 0.066; paired t = -2.62, p = 0.011) (Figure 5), indicating the evolution of cost compensatory

mechanisms. We observed higher mean adaptation costs in more complex environments (>1D) relative to single stressor environments (1D) at both T7 (t = 5.23, df = 54.544, p<0.01) and T15 (t = 4.26, df = 43.714, p < 0.01). The fitness costs associated with adaptation varied among stressors and across time points. At T7, adaptation to heat stress imposed the highest fitness cost in YPD (F(1,55) = 7.93, p < 0.01), while at T15, adaptation to antifungal resulted in the greatest fitness cost in YPD (F(1,55) = 4.77, p = 0.033).

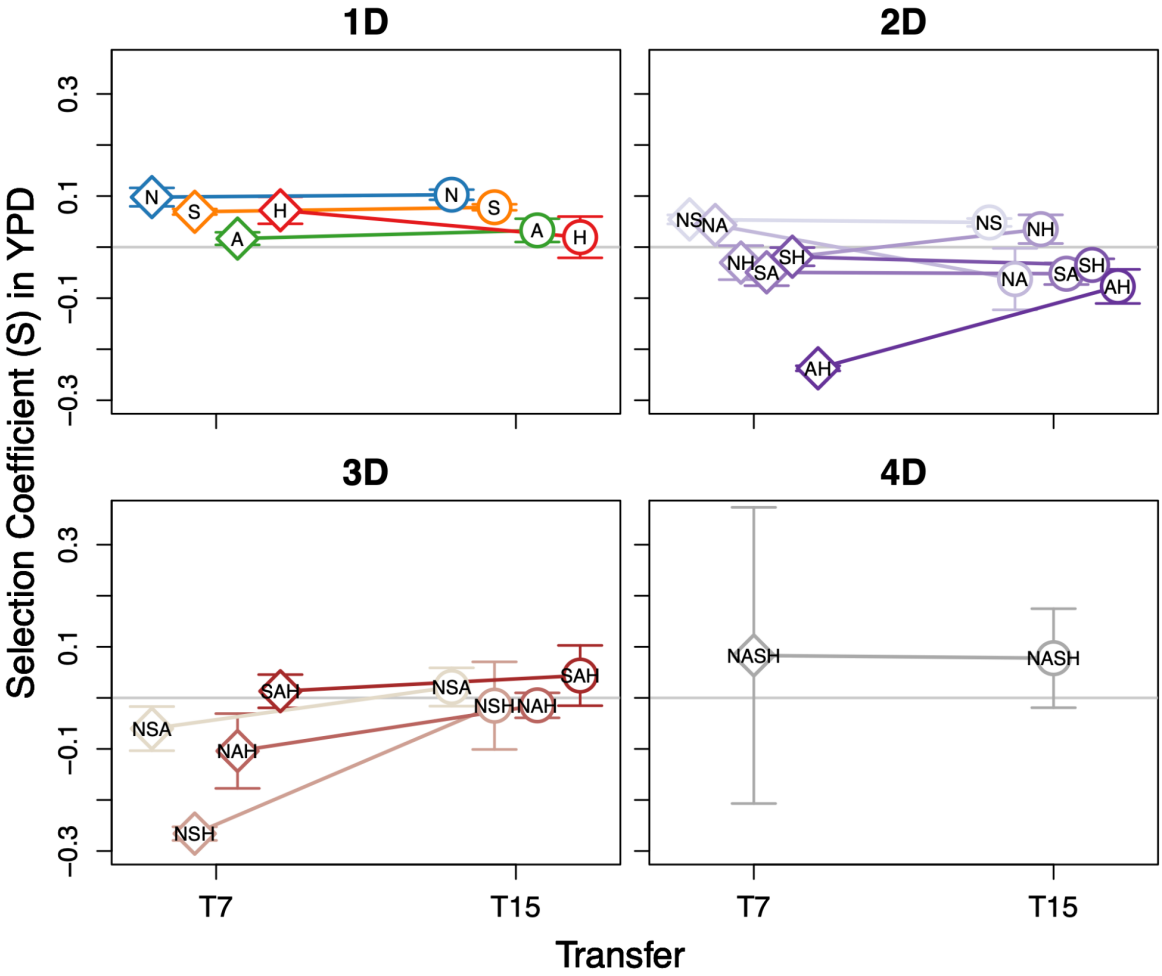

Figure 5. Cost of adaptation in the ancestral environment (YPD) for each evolved population, partitioned by environmental complexity level (1D–4D). Estimated selection coefficients are shown as diamonds (T7) and circles (T15) with bars as standard deviations. The grey line represents a selection coefficient of 0. T0 is excluded for visualization purposes.

237 **Genomic dynamics and basis of adaptation characterized by few, but pleiotropic,**
238 **mutations**

239 We identified 228 SNPs and 57 INDELs across all timepoints and populations in our
240 experiment. Populations varied moderately in SNP and INDEL number by T15 (mean =
241 3.91, SD=3.55), with some populations seemingly containing no mutations (see Discussion)
242 while the highest number of mutations (n=18) was in the antifungal-adapted population,
243 A2. Despite clear instances of phenotypic evolution in most populations (Figure 2),
244 mutational sweeps were rare. By T7, 21.6% (13/60) of populations had at least one
245 mutation fixed or nearly fixed with an allele frequency greater than 0.80, and this
246 proportion increased to 31.6% (19/60) by T15 (Figure 6). The probability of observing
247 sweeps by T15 was stressor-biased, where sweeps were more associated with evolution in
248 antifungal (β=0.676, p<0.001) than salt and starvation (both β=0.363, p=0.037), and heat
249 (β=0.176, p=0.305). Although we do not formally quantify selection (due to hitchhiking
250 mutations) at the genomic level, predicted effects of mutations by snpEff showed that the
251 mutations that did sweep were primarily mutations of at least moderate putative effect
252 (Figure S5). We additionally observed some signals of clonal interference, especially
253 between the mutations conferring antifungal resistance, where initially high frequency
254 mutations (at T7) had decreased in frequency by T15, likely in response to the acquisition
255 of a new mutation (e.g. A3, NA3, NASH4). Of the 129 high frequency mutations at the
256 midpoint of the experiment, 83 (64%) mutations across 32 (of 60) lines decreased in
257 frequency by at least 10% by the end of the experiment.

258 We also found larger structural variants during experimental evolution by
259 identifying chromosomes or regions within a chromosome with elevated coverage relative
260 to the genome-wide or chromosome-level sequencing depth, respectively. At the
261 chromosome level, we observed that chromosome 12 showed consistent patterns of copy
262 number gain (aneuploidy) across several line replicates (NSA1, NSA3, NAH1, SAH1,
263 NASH1) while chromosome 14 was elevated in one replicate (also in NAH1) (Figure S6).
264 Chromosome 12 contains genes related to pleiotropic drug resistance (PDR8, TOP1, CIS1),
265 osmotic stress (FPS1, RCK2, STE11, SGD1, SSK1), glucose limitation (SSA2, YPT2, GSY2,
266 ECM30, FBP1), and heat stress (SSQ1, SYM1, GSY2, HSP60,HSP104, SSA2). Chromosome 14

267 contains genes for osmotic stress (VAC7, POR1, SSK2, INP52,SKO1, FIG4), pleiotropic drug
268 response (MKT1,HCH1, PDR16,HDA1), and heat stress (HCH1, WSC2, HDA1, YDJ1,
269 NMA111).

270 Within individual chromosomes, only two partial CNVs were identified (Figure S7).
271 The first in the NAH1 population between 90kb–150kb on Chromosome 3 (spanning 35
272 genes) at both T7 and T15, and the second in SAH2 only at T7, between 46kb–70kb on
273 chromosome 15 (spanning 14 genes). The partial CNV in NAH1 contains genes related to
274 salt homeostasis (SAT4, RVS161), and the CNV in SAH2 contains genes related to glycolysis
275 (PFK27) and transcriptional response to glucose starvation (RTC1), among others.

276 We found that populations typically contained mutations whose putative effects
277 (based on gene ontology terms, see Methods) matched their evolved environment (Figure
278 6). In particular, we found that almost all populations evolving in the presence of antifungal
279 (27/32) acquired mutations in at least one of three genes (PDR1, PDR3, and PDR5)
280 encoding for pleiotropic drug response factors or transporters (Akache et al. 2004) and are
281 known to confer resistance to fluconazole (Spampinato and Leonardi 2013). Furthermore,
282 antifungal-related mutations are often the first to appear and rise in frequency in these
283 populations, suggesting that adaptation to antifungal is more mutationally accessible (i.e.,
284 simpler genetic basis and possibly higher genome-wide mutation rate) than other
285 stressors.

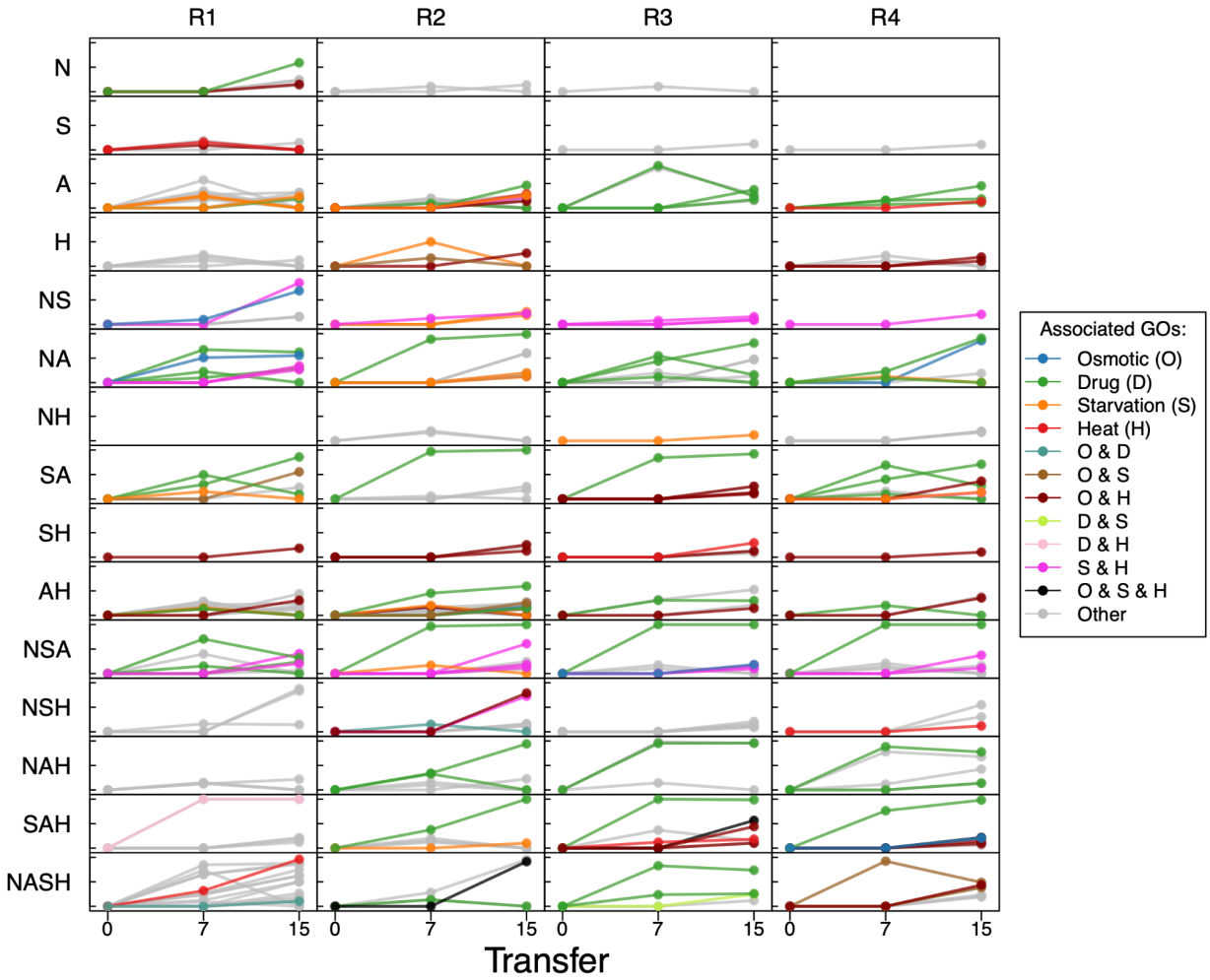

Figure 6. Allele frequency dynamics in evolved lines. Points represent allele frequencies at time points at T0, T7, and T15. Points are colored by association with general gene-ontology terms: Response to osmotic stress (O), response to starvation (S), drug response (D), and response to heat (H). Some mutations have overlapping GO terms, and are colored separately for each type of overlap. Replicates are designated as R1–R4.

Despite abundant mutations with clear associations to the environment they appeared in, many genes targeted by mutation are likely pleiotropic, affecting many biological processes (Figure 7A). Here we use the number of gene-ontology terms (pruned for redundancy using R package `rrvgo` v1.12.2) for each mutation as a proxy of pleiotropic effects. Strikingly, we observed that the pleiotropy of mutated genes increased as complexity increases (β=1.162, p=0.028, Figure 7B).

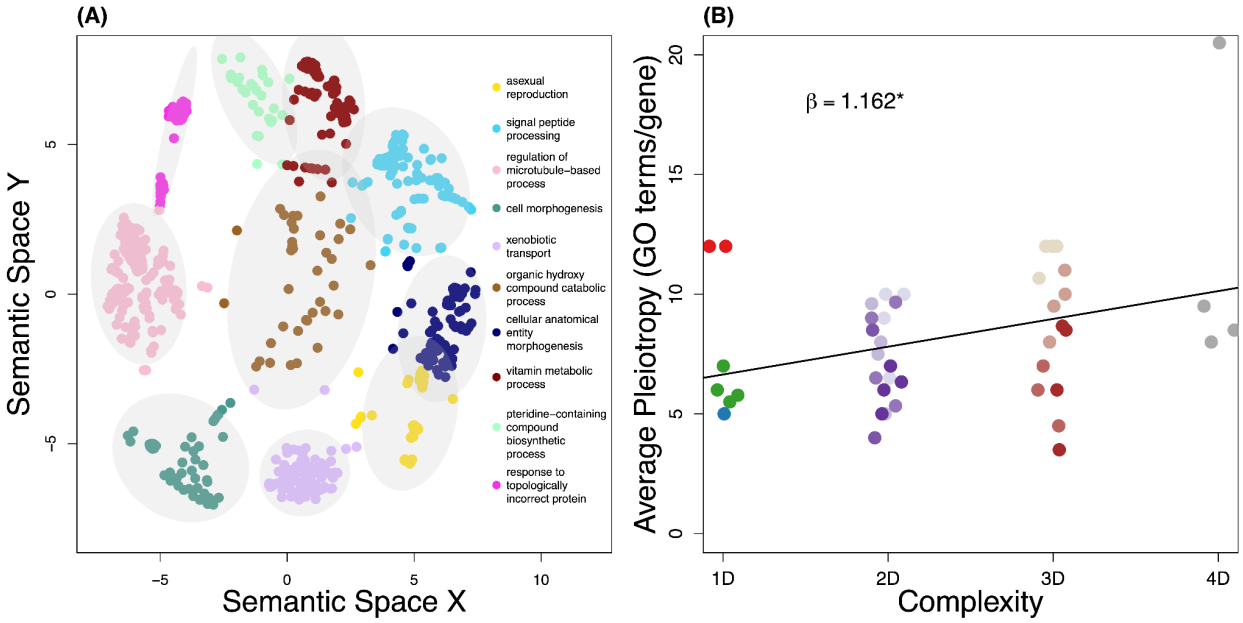

Figure 7. Pleiotropy of genes mutated during experimental evolution. (A) Visualization of the types and number of biological processes associated with all mutations observed during experimental evolution. Gene ontologies were pruned for redundant terms based on semantic similarity using the R package rrvgo and clustered for visualization with k-means clustering (k=10). For each cluster, the term with the lowest dispensability score is shown. (B) Average number of GO terms associated with gene mutations in each level of environmental complexity at the end of experimental evolution (T15). GO terms were first clustered by semantic similarity using R package rrvgo to reduce redundancy. To account for mutations which may not contribute to adaptation, we consider only those which have increased to an allele frequency of at least 20% in any population. The slope of the regression is plotted and shown. The asterisk indicates a significant slope.

Parallel mutational targets across levels of environmental complexity

We observed high genetic parallelism (Figure 8), with 44/60 lines sharing at least one genic mutation with another independent line. These recurrent mutational targets consisted of 20 genes (13.89% of the 144 total genes). The PDR family of genes, involved in pleiotropic drug response, showed the most prominent mutations, with nearly all lines evolved in the presence of fluconazole (27/32) acquiring mutations in either PDR1, PDR3, or PDR5. PUF3 had the second-highest number of shared mutations, primarily appearing in populations exposed to high heat (particularly in all four SH replicates). Notably, PUF3 null mutants are associated with innate heat tolerance (Harris et al. 2005; Jarolim et al. 2013). Although high heat imposed the lowest stressor effect (Figure 1C), heat tolerance may be easily accessible through loss-of-function mutations of PUF3.

323 At the nucleotide level, 10 point mutations were shared between two or three
324 independent lines by the end of the experiment (Figure S8). Consistent with the genic-level
325 findings, the most common recurrent SNP mutations were in PDR1 and PUF3. Both PDR1
326 and PUF3 showed recurrent mutations at two different positions. Shared SAC3 mutations,
327 associated with yeast bud and cell size morphological changes (Watanabe et al. 2009;
328 Jorgensen et al. 2002) and possible heat resistance (Jani et al. 2009), were observed in
329 NSH1 and NSH3. We also observed shared mutations in several other genes with known
330 functions: SAC3, associated with bud and cell size morphological changes and increased
331 heat resistance in S288c, appeared in NSH1 and NSH3; YAK1, encoding a regulator of
332 glucose-deprivation stress response (Moriya et al. 2001), in NS1 and NS3; and SOD1, where
333 mutations double yeast lifespan during stationary phase (Harris et al. 2005), in SH2 and
334 SAH4. The remaining shared point mutations occurred in genes of unknown function:
335 MLF3 (in S3 and S4), DFP1 (in NSH2 and NASH4), and YDL228C (in NS1 and SH3).

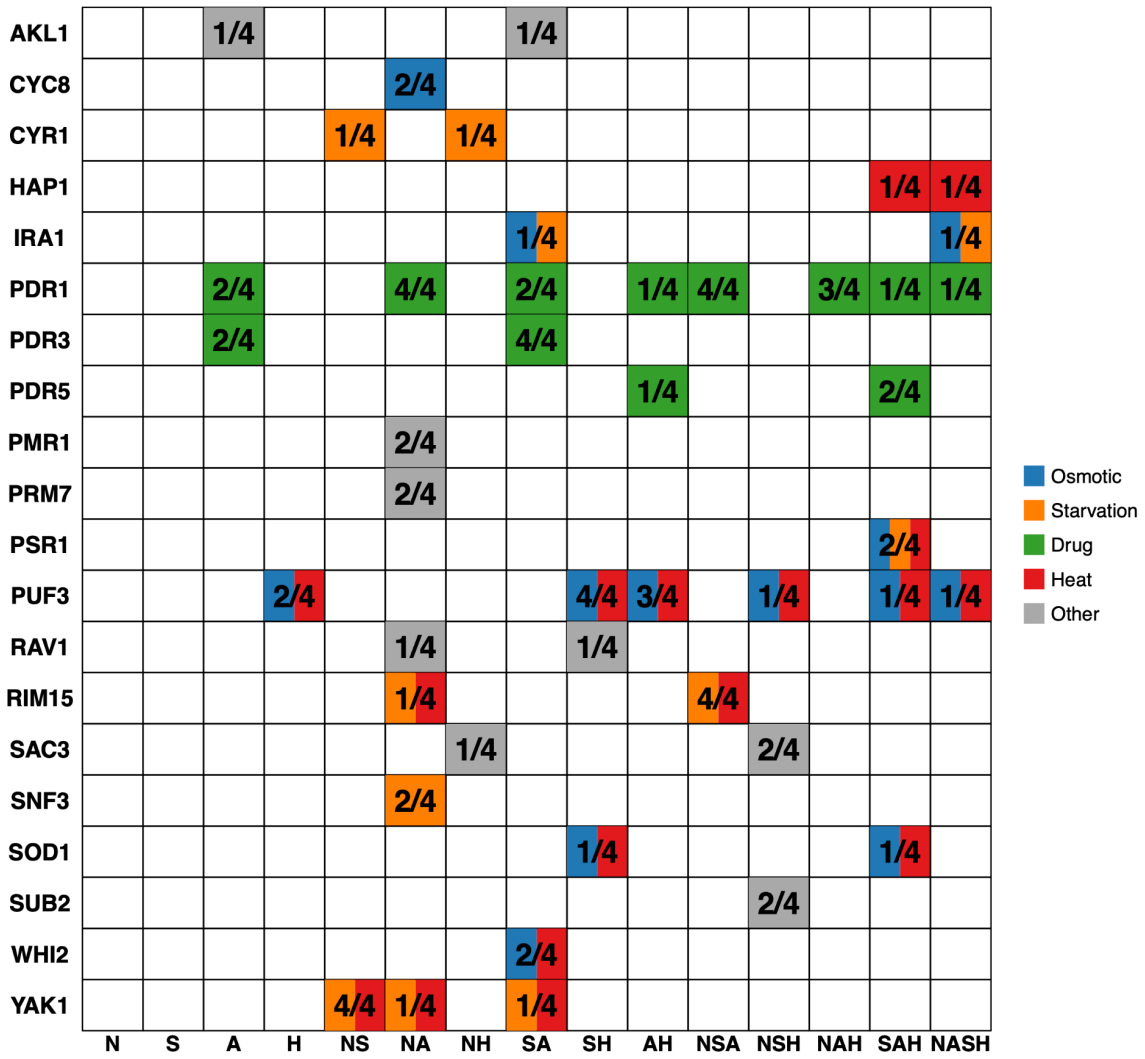

Figure 8. Recurrent mutations in the same gene across independent evolved populations. Shared genic mutations are colored by the parental GO category, white indicates no shared mutation. The fraction indicates the number of line replicates (of four total) which harbor that gene mutation.

Gains and losses of putative compensatory mutations during trade-off evolution

We found several fitness trade-offs at T7 where populations were maladapted to one of the individual components of their complex environment. However, most trade-offs resulting in negative fitness at T7 had been compensated for by T15 such that relative fitness had at least increased to nearly neutral (≈0) or positive values (Figure S2, Figure S3). We further investigated putative mutations concomitant with the largest fitness compensations (Supplementary Table 1).

349 In lines with the greatest compensatory evolution, fitness changes between T7 and
350 T15 typically were more often concomitant with gaining additional *de novo* mutations
351 rather than the loss of *de novo* mutations. Many of these new mutations were not clearly
352 related to a biological function associated with the tested single-stressor. Additionally,
353 when mutational losses occur, the functions of the affected gene are more likely to be
354 associated with a different stressor than the one tested. For example, the NASH1 line had
355 some of the greatest compensatory evolution in both salt (fitness change from S_{T7}=-0.21 to
356 S_{T15}=0.12) and high heat (S_{T7}=-0.38, S_{T15}=-0.14) conditions. While the mutations gained
357 between the midpoint (T7) and end (T15) of experimental evolution were not directly
358 related to either salt or heat stress (affecting protein phosphorylation [SKY1], vacuolar
359 protein catabolism [PRC1], and mitochondrial nuclease and mRNA processing [BI2 and
360 BI3]), the single mutation lost was in CSG2. CSG2 encodes a regulatory subunit for
361 mannosylinositol phosphorylceramide synthase, which works with ergosterol to maintain
362 cell wall integrity. Notably, the mechanism of fluconazole action involves inhibiting
363 ergosterol synthesis, thereby disrupting cell wall permeability (Spampinato and Leonardi
364 2013). The loss of the CSG2 mutation corresponded with decreased antifungal fitness in
365 NASH1 from S_{T7}=0.25 to S_{T15}=0.15. Similar patterns were found in lines such as NSA3 (loss
366 of FCY2, which shows cross-resistance to fluconazole) and NSA4 (loss of TEC1, which
367 prevents penetration of fluconazole into the cell wall of *Candida albicans*).

368 This general pattern of compensatory evolution also occurred in cases not involving
369 antifungal resistance, though to a lesser extent. For instance, the NSH2 line demonstrated
370 some of the greatest compensatory evolution under both glucose starvation (S_{T7}=-0.29 to
371 S_{T15}=0.19) and heat stress (S_{T7}=-0.23 to S_{T15}=0.1). NSH2 gained mutations in genes
372 associated with chromosome segregation (OKP1) and mitotic recombination (THP2). While
373 NSH2 acquired mutations potentially relevant to the tested stressors, including PUF3,
374 which has been linked to heat shock response, and IRA2, which regulates cAMP levels
375 during nutrient limitation, NSH2 lost a mutation in AUR1, a gene associated with
376 hyperosmotic stress resistance. Unlike in antifungal populations, the loss of AUR1 did not
377 decrease NSH2's salt tolerance (S_{T7}=0.1 to S_{T15}=0.25). These observations support a two-
378 stage evolutionary process in which adaptation occurs initially to a primary stressor that

379 compromises resistance to secondary stressors, followed by evolutionary refinement that
380 enhances overall stress resilience while sometimes reducing the effectiveness of the initial
381 adaptation (as seen with antifungal resistance).

382 Discussion

383 Natural environments in which evolution occurs are immensely complex, with variation
384 across multiple axes and timescales. While experiments in simplified environments in the
385 laboratory have produced key insights about fundamental evolutionary processes and
386 mechanisms, they have been criticized for lacking ecological realism, potentially limiting
387 our understanding of evolution in natural populations (Waldvogel et al. 2020; Bergelson et
388 al. 2021; Venkataram and Kryazhimskiy 2023; Zelnik et al. 2024). As a stepping-stone
389 between simplified laboratory environments and nature, we adapted populations of yeast
390 to a full-factorial combination of four stressors to assess the mode and dynamics of
391 adaptation as environmental complexity increases. Our results demonstrate that
392 adaptation to complex environments imposes trade-offs between traits whose dynamics
393 can rapidly evolve. The order of adaptation to stressors was biased first by mutational
394 accessibility and subsequently by the strength of selection. Trade-offs imposed fitness costs
395 not only in stressors that had been simultaneously selected for, but also in stressors that
396 the evolving lines had never been exposed to, and even in the initially benign ancestral
397 environment. However, initial trade-offs were often compensated through mutational fine-
398 tuning, with mutations of greater pleiotropic effect arising in more complex environments.

399 Dynamics and genetic basis of adaptation to complex environments

400 We observed rapid fitness increases over the course of 15 serial transfers in almost all
401 treatments and lines (Figure 2). While many lines had plateaued by the experiment's
402 midpoint, those in higher-dimensionality environments continued to gain fitness between
403 T7 and T15, albeit at a reduced rate. This pattern of initially rapid adaptation followed by a
404 fitness plateau aligns with previous studies of microbial evolution from *de novo* mutations
405 (Wiser, Ribeck, and Lenski 2013; Johnson et al. 2021). The continued evolution of
406 improved fitness in complex environments likely stems from two factors. First, populations

407 experiencing multiple stressors may start further away from their fitness optimum as a
408 result of increased environmental stress and require more time and mutational steps to
409 approach the optimum (Hoffmann and Hercus, 2000). Adaptation to complex
410 environments may also have a more polygenic genetic basis (Anderson et al. 2014),
411 requiring additional time to acquire the necessary mutations.

412 At the genomic level, we observed the appearance and subsequent rise in frequency
413 of SNPs, INDELs, and copy number variants during evolution (Figure 6, Figure S6, Figure
414 S7). Genomic evolution in our lines was characterized by few mutational sweeps and
415 moderate repeatability. The paucity of sweeps may be due to the effects of clonal
416 interference, which frequently occurs in large populations such as in our experiment (Park
417 and Krug 2007), which can slow down the rate of genomic adaptation (Miralles et al. 1999;
418 Hughes et al. 2012). Lines adapting to the presence of fluconazole were notable exceptions,
419 often exhibiting rapid sweeps and parallel gene mutations. This exception may be
420 attributed to the simple genetic basis of antifungal resistance in conjunction with a
421 heightened mutational supply. Not only is fluconazole known to increase the rate of DNA
422 damage (Silva et al. 2019; Yüzbaşioğlu et al. 2008; Ribeiro et al. 2022), but the most
423 common mode of evolution for antimicrobial resistance typically comes from either loss- or
424 gain-of-function mutations in a single gene (Bavro, Conn, and Davies 2019). This is
425 reflected in the recurrent mutations found in the PDR family of genes, in which mutations
426 have been shown to increase the efflux of azoles in other studies of yeast by up to 40 times
427 (Wang et al. 2022).

428 Many genes targeted by mutations during experimental evolution were associated
429 with multiple biological processes not immediately related to the environmental
430 components. We observed that mutations associated with a greater number of different
431 biological processes arose in environments of higher complexity. This suggests that
432 acquiring mutations with pleiotropic effects, which may perform multiple functions
433 (though less than optimally), results in higher fitness than acquiring multiple mutations in
434 different genes that each affect only one particular trait, or that mechanistic constraints
435 exist between genes of specialized functions. However, since greater pleiotropy was

436 observed only at the end of the experiment, in conjunction with an order bias of adaptation
437 and patterns of compensatory evolution to individual stressors (see below for further
438 discussion), this suggests that adaptation first proceeds by mutations in genes of
439 specialized function, whose functions are fine-tuned by mutations of pleiotropic effect.

440 **Trade-off evolution between environmental stressors**

441 Fitness trade-offs were abundant across all environments and conditions. Our fitness
442 assays showed that no line evolving in a complex environment was able to reach the same
443 level of fitness in all respective individual environments as the populations evolved solely
444 in those single stressors. When present, the order of adaptation to environmental
445 components was biased primarily towards antifungal resistance, which often involved
446 negative fitness consequences towards other stressors (heat in particular). Although
447 fluconazole did not impose the strongest selection of the four individual stressors, its
448 resistance is easily acquirable due to a simple genetic basis. Interestingly, the next-most
449 prioritized adaptation was salt resistance, which did impose the greatest selection strength,
450 but is a highly polygenic trait (Dhar et al. 2011). This indicates that the ease of mutational
451 accessibility to antifungal resistance drives early adaptation and trade-off dynamics, but
452 the strength of selection determines adaptive dynamics among treatments in which the
453 basis of adaptation are more polygenic, both consistent with mutations of greater effect
454 size fixing first in other evolution experiments (Elena and Lenski 2003; Lang et al. 2013).

455 While resistance to starvation and particularly heat showed the greatest negative
456 trade-offs at the midpoint of the experiment, these trade-offs were often nullified or even
457 reversed by the end of the experiment. Interestingly, in the cases where we observed the
458 greatest compensatory evolution (i.e. where maladaptation was entirely negated or even
459 reversed), mutations that were gained or lost did not necessarily have a direct connection
460 to the stressor in which compensation was found. Rather, affected genes were often related
461 to a stressor to which the line was already adapted, supporting models that predict most
462 adaptation signatures are linked to compensatory evolution rather than novel function
463 acquisition (Pavlicev and Wagner 2012; Zhang et al. 2024).

464 Despite the abundance of trade-offs, some populations still managed to adapt to
465 multiple stressors simultaneously. While a scan of first-step mutations in yeast have shown
466 that mutations which simultaneously increase fitness across multiple traits is possible (Li,
467 Petrov, and Sherlock 2019), this does not seem to be the primary mode of initial adaptation
468 in our lines. Though uncommon, some lines evolved in complex environments even showed
469 fitness surpassing that of specialist (1D) lines in at least one of the respective environments
470 (Figure S2), indicating that some mutations had strongly positive pleiotropic effects in
471 complex environments. Previous studies in DNA bacteriophages have shown that when
472 selection in complex environments is particularly strong, traits constrained by antagonistic
473 pleiotropy may acquire mutations which enhance multiple traits concurrently (McGee et al.
474 2016), thus overriding the trade-off costs associated with a complex selective environment.
475 As many of these instances of adaptation greater than the specialist occur in either the 3D
476 or 4D treatments, these populations may be forced to exploit mutations that have enhanced
477 positive pleiotropy under the threat of extinction. While not quantified during
478 experimental evolution, several lines at higher complexities (3D and 4D) experienced
479 extinction at the beginning of the experiment and were restarted.

480 **Trade-off evolution of novel and ancestral environments**

481 Trade-offs in non-selected ("novel") environments were less prevalent and showed
482 different, sometimes non-reciprocal, patterns across environments. For example, by the
483 end of the experiment, the average fitness across all four replicate lines in each of the seven
484 treatments containing fluconazole showed either no adaptation or maladaptation when
485 exposed to novel fluconazole. Yet, the average fitness across replicates in five of the seven
486 lines containing fluconazole exhibited latent adaptation to novel heat stress, including the
487 line exposed to fluconazole alone. This asymmetry likely reflects the specificity of
488 adaptation to each environmental component. Fluconazole adaptation in our lines
489 commonly occurred through mutations in PDR genes, which specifically affect the efflux of
490 azoles. However, fluconazole's downstream effects disrupt cell wall stability (Spampinato
491 and Leonardi 2013). Adaptation to the other stressors (salt, heat, and starvation) can
492 involve changes to cell wall permeability and stability (Bermejo et al. 2010; Piper 1995;
493 Hohmann 2002), and adaptive mutations for these stressors may thus have antagonistic

494 pleiotropic effects for fluconazole resistance. Contrary to the negative pleiotropic effects
495 found with fluconazole, the other three non-selected environments showed largely positive
496 pleiotropy, likely because adaptations to these stressors share stress response mechanisms
497 that provide cross-protection.

498 In a previous experimental evolution study, *E. coli* evolved in the presence of
499 multiple concurrent antibiotics were more likely to acquire pleiotropic mutations that
500 allowed them to gain novel resistances to previously unexposed antibiotics (Karve and
501 Wagner 2022). However, contrary to these results, we observed that higher degrees of
502 environmental complexity were associated with reduced fitness to novel stressors. This
503 discrepancy may again result from the specificity of resistance mechanisms between the
504 diverse stressors used in our study (salt, heat, starvation, antifungal) versus different types
505 of antibiotics, which in contrast often involve more limited mechanisms such as efflux
506 pumps or cell permeability changes.

507 Local adaptation may result in the maladaptation of a population to its ancestral
508 environment. Indeed, trade-offs in the ancestral environment were prevalent, and also
509 varied across levels of environmental complexity. Lines adapted to single stressors
510 generally exhibited increased fitness in the ancestral environment and maintained these
511 gains through the end of the experiment. In contrast, lines adapting to multiple stressors
512 initially showed reduced fitness in the ancestral environment. While these costs often
513 decreased by the end of the experiment, complete nullification or reversal of costs rarely
514 occurred. This pattern aligns with empirical evidence that steeper environmental clines
515 induce greater costs of adaptation than shallower clines (Collins and de Meaux 2009). Our
516 observed diminishing costs of adaptation over time further support a compensatory mode
517 of adaptation, where selection acts against antagonistic pleiotropic effects (Pavlicev and
518 Wagner 2012).

519 **Conclusions**

520 Here, we assessed both the phenotypic and genomic evolutionary dynamics in lines
521 adapting to simple and complex environments containing multiple selective agents (full-

522 factorial combinations of antifungal, heat, stress, and starvation). Our work highlights
523 avenues in which patterns of adaptation and trade-off evolution can be predicted.
524 Populations adapted rapidly to concurrent multifarious selection pressures, yet adaptive
525 dynamics were primarily determined by the order of mutational accessibility. The
526 acquisition of antifungal resistance typically arose first, and through remarkably similar
527 pathways across all levels of environmental complexity. A leading strategy for the combat
528 of both microbial infections and agricultural pests is to apply multiple antimicrobial drugs
529 or pesticides at the same time (REX Consortium 2010). Our results indicate that unless the
530 selection pressure from these multiple drug treatments is great enough to quickly
531 exterminate a pathogenic or pest population, resistance will likely evolve. Further,
532 antifungal resistance developed by similar mechanisms regardless of environmental
533 complexity (but see (MacLean et al. 2010) for cases in which environmental context does
534 alter the genetic basis of resistance). We also observed that evolution to complex
535 environments led to a greater cost of adaptation to novel and ancestral environments. This
536 suggests a concerning pattern that as populations adapt to multiple stressors
537 simultaneously (e.g., warming temperatures and increased pollution), they may become
538 less able to maintain high fitness under different conditions. Further, our findings indicate
539 that as populations experience an increasing number of anthropogenic forces (Hendry,
540 Gotanda, and Svensson 2017), their susceptibility to further habitat change may increase
541 due to these accumulated adaptation costs. In extreme cases, habitat restoration may even
542 decrease the fitness of a population, such as in plants adapted to heavy-metal uptake from
543 mines (Hickey and McNeilly 1975).

544 Importantly, our findings indicate that adaptive dynamics in simple environments
545 cannot be used to reliably predict outcomes in more complex ones. As environmental
546 complexity increases, both the trajectory and genetic architecture of adaptation shift,
547 introducing pervasive trade-offs, pleiotropic constraints, and compensatory dynamics that
548 are rare or absent under single-stressor selection. These patterns highlight not only the
549 need to study adaptation in ecologically realistic, multidimensional environments, but also
550 the importance of understanding the underlying mechanisms that shape these responses.
551 In particular, knowing whether adaptive mechanisms are stressor-specific or broadly

552 acting will be essential for predicting the degree and direction of pleiotropy, and the
553 constraints that emerge when multiple selective forces act simultaneously.

554 Materials and Methods

555 Strain information and environments

556 All strains used in this study were derived from a S288c background. The ancestral
557 population was a haploid LJY170 strain (*MATa, hisΔ200, trpΔ63*, donated by Lars Jansen,
558 Oxford University; see (Stajic, Perfeito, and Jansen 2019). A fluorescent strain RSY328
559 (*MATa, hisΔ200, trpΔ63, chrV 115940-116010::NatMX6-mCitrine*) was used as a reference
560 for flow cytometry fitness measurements (see below). RSY328 was constructed by
561 integration of a NatMX6-mCitrine cassette into an intergenic region on chromosome V,
562 creating a deletion of the sequence spanning the positions 115,940bp to 116,010bp
563 without affecting ORFs of neighboring genes. The NatMX6-mCitrine construct was
564 amplified from a pRS5 plasmid, designed by insertion of mCitrine from pFA6a-ACT1-
565 ymCitrineM233I::HISMX6 into a pAG25 backbone using HindIII and BglII restriction
566 enzymes.

567 Four stressors were used in full-factorial combinations, resulting in a total of 15
568 environments: 0.8M NaCl, 0.5% Glucose YPD, 37°C , and 20μg/ml of the antifungal
569 Fluconazole (Figure 1A). Populations not grown in heat stress (at 37°C) were grown at a
570 benign 25°C. To quantify the potential selective pressure of each environment, we grew the
571 ancestral population in each environment for 24h from an initial optical density of 0.02 at
572 600nm (OD600) and measured the reduction in final OD600 relative to the OD600 in the
573 base yeast extract peptone dextrose (YPD; 1% yeast extract, 2% peptone, 2% dextrose)
574 medium at 25°C (n=3) (Figure 1B).

575 Experimental evolution

576 At the start of experimental evolution for each environment, an individual colony was
577 isolated to serve as the ancestral population, by streaking from frozen stock culture and
578 growing on YPD agar plates (2% agar), for 72 hours. Cells were inoculated in 5ml liquid

579 YPD for 24 hours at 25°C and 200rpm. Subsequently, four replicates were inoculated in
580 5mL of each of 15 different selective environments, serving as biological replicates. Starting
581 population size across all replicates was standardized to OD600 of 0.02 using a BioTek
582 EPOCH2 microplate reader. Cultures were grown in their respective environments at 200
583 rpm. Every 48 hours 2% (100µl) of the culture was transferred to fresh media. In total, 15
584 transfers were completed and samples were preserved in 44% glycerol at -80°C for
585 phenotypic and genomic analyses (Figure 1C).

586 **Fitness assays**

587 Flow cytometry competition assays were performed using a Luminex Guava easyCyte. A
588 fluorescently labeled strain (RSY328; MATα, hisΔ200, trpΔ63, chrV 115940-
589 116010::NatMX6- mCitrine) derived from the ancestral LJY170 background was used as a
590 reference strain. The fluorescent strain was streaked on YPD agar plates and an individual
591 colony was inoculated at 25°C and 200 rpm shaking for 24 h prior to measurement in the
592 flow-cytometer. Frozen samples of the evolved populations at transfer 7 (T7) and 15 (T15)
593 were thawed and 100µL was inoculated into 5mL of the corresponding selective
594 environment for 24 hours. For each evolved population, three technical replicates were
595 tested. After overnight growth, evolved populations and the fluorescent strain were mixed
596 in a 1:1 cell ratio so that the final OD of the mixture was 0.02. Competition assays were
597 performed in every single-stressor treatment, including the ancestral YPD medium, as well
598 as in the relevant multi-stressor treatment. Prior to measurement with flow cytometry,
599 mixed cultures were diluted to an OD of 0.005 and suspended in PBS (pH 7.4) solution. The
600 count of ancestral fluorescent and non-fluorescent evolved cells were measured using flow
601 cytometry after the initial mixing (0 hours) and after 48 hours to determine the change in
602 proportion of evolved to ancestral cells (Supplementary Figure 9).

603 The relative fitness (selection coefficient) of the evolved strain to the ancestor was
604 calculated as the slope of the linear regression of the log ratio of cell numbers ($\frac{evolved}{ancestral}$)
605 and the number of cell doublings between time points (0 hours and 48 hours). To account
606 for any possible fitness effects of the integrated fluorescent construct, we normalized the

607 selection coefficient values by the difference in fitness between fluorescent and non-
608 fluorescent ancestor strains for each environment.

609 **Sequencing and bioinformatic processing**

610 To culture cells for sequencing, 100µL of the frozen evolved population were inoculated in
611 5ml of the corresponding environment for 24 hours with shaking at 200 rpm.
612 Approximately 1 ml of the culture was used for DNA extraction. DNA was extracted from
613 the ancestral stock population and whole population samples at T7 and T15 of
614 experimental evolution. The isolation of gDNA was conducted either by using a column-
615 based method following manufacturer's instructions (NucleoSpin Microbial DNA kit,
616 Macherey-Nagel, Du¨ren, Germany) or an automated system (King Fisher Duo Prime
617 System, Thermo Scientific, MA, USA) in combination with a magnetic bead-based method
618 (Mag-Bind Blood & Tissue DNA HDQ kit, Omega Bio-Tek, GA, USA). Quantification of gDNA
619 samples was conducted using a fluorometric method (Qubit, Thermo Scientific, MA, USA)
620 and library preparation was conducted either in the laboratory (DNA Prep Tagmentation
621 kit and IDT (UD) indexes (Illumina, Hayward, CA, USA) or at the National Genomics
622 Infrastructure Sweden (NGI) (DNA Flex library kit, Illumina, Hayward,CA, USA). The
623 libraries were sequenced at the NGI on an Illumina MiniSeq platform with a 2x150 bp
624 paired-end setup using a MiniSeq Mid Output kit or on an Illumina NovaSeq6000.
625 Estimated average genome-wide coverage per sample ranged from 37.29–416.66x.
626 Sequence data are submitted to ENA (accession number to be released upon acceptance).

627 The quality of sequencing reads after trimming with Trimmomatic v0.36 were assessed
628 with FastQC v0.11.9 and MultiQC v1.11. The reference strain used was S288c (R64, GCF
629 000146045.2). Reads were aligned using BWA MEM v0.7.17 with the following parameters:
630 -k 20 -r 1.3 -M. Reads were sorted and merged with samtools v1.17 (Danecek et al., 2021),
631 and deduplicated with Picard v2.23.4 (Broad Institute). To call variants, we used GATK
632 v4.1.4.1 HaplotypeCaller with best practices (McKenna et al., 2010). The raw VCF was
633 filtered with the following criteria: QD < 0.5, QUAL < 20. Regions of the genome which were
634 not uniquely mapping to itself were then filtered out using GenMap v2.4.1 (K31, E2)
635 (Pockrandt et al., 2020), retaining 3070 variants. Sites were further filtered out if: i)

636 variants existed in the ancestral population at <5% frequency in all populations and time-
637 points; ii) had less than 20 reads in greater than 20% of the total samples; iii) had more
638 than 10% of samples missing data, or iv) were found in more than 10% of samples. After
639 filtering, 1048 variants remained. These variants were subsequently manually inspected in
640 the Integrative Genome Viewer v2.16.0. Sites mapping to multiple locations, and
641 homopolymeric or tandem repeat regions were discarded, resulting in a final set of 228
642 SNPs and 57 INDELs. Allele frequencies were calculated using the ratio between alternate
643 and total allele depth. For each mutation, we estimated its putative effect size using snpEff
644 (Cingolani et al., 2012), which uses the annotation of the reference strain to predict
645 functional effects based on the type of mutation observed (e.g. synonymous, missense,
646 frame-shift, etc).

647 Mutations in genic regions were associated with GO terms from the *Saccharomyces*
648 *cerevisiae* Ensembl BioMart database using the R library package biomaRt (v.2.42.1). If the
649 GO term of a mutation was found to be a lower-level GO term under one of these parent GO
650 terms, it was grouped in the parent GO term category. Mutations which fell under multiple
651 parent GO terms were assigned to each associated category. We then manually verified
652 from gene entries in the Saccharomyces Genome Database (Cherry et al. 1998) that GO
653 terms were accurately assigned to mutations for the four main GO term groups which
654 characterize our selective treatments: osmotic stress (GO:0006970), response to starvation
655 (GO:0042594), drug response (GO:2001023), or response to heat (GO:0009266).

656 **Copy number variation**

657 We assessed potential partial- and whole-chromosome copy number variations (CNVs) in
658 each evolved population. For partial CNVs, we calculated relative depth per population
659 across 5kb non-overlapping windows compared to mean depth for each chromosome
660 individually. Sites which differed by more than 20% of the mean relative depth per
661 chromosome in the ancestral population were excluded for analyses as likely repetitive
662 regions. Some samples had non-uniform read depth across chromosomes, where the
663 centers of chromosomes had lower depth than the ends, leading to a wide U-shape pattern.
664 This is a common pattern described in previous work, but is not associated with average

sample coverage, flow-cell, or sequencing machine (Abbey et al. 2014; Ament-Velásquez et al. 2022; Sun et al. 2023). For every sample we fit a LOWESS curve for each chromosome based on relative depth by distance-to-chromosome-end. Relative depths were divided by the output of the LOWESS function to normalize this U-shaped pattern in the data. To detect whole-chromosome aneuploidies, we calculated relative mean depth per chromosome compared to the mean whole-genome read depth. We identified putative CNVs as windows or chromosomes which had a change in relative depth of greater than 20% from the ancestor to either subsequent time point (T7 or T15).

Data Availability

Data is available at Figshare (doi upon release:10.6084/m9.figshare.29149616). The raw read data will be available at the European Nucleotide Archive upon acceptance. All scripts and data fall under a CC0 1.0 Universal (CC0 1.0) license.

Code Availability

Peer review link to code and data: https://figshare.com/s/6dd76de272b899ce77f0

Acknowledgements

We would like to acknowledge Mario Walthert and Ciaran Gilchrist for assisting in growth-curve and flow cytometry measurements. The computations and data handling were enabled by resources in project [NAISS 2023/23-487] provided by the National Academic Infrastructure for Supercomputing in Sweden (NAISS) at UPPMAX. This work was supported by the Swedish Research Council (2017-04963 and 2022-03427 to RS) and the Knut and Alice Wallenberg Foundation (2017.0163 to RS). CB is supported by “la Caixa” Foundation (ID 100010434), under agreement (LCF/BQ/AA16/11580051), by the Fonds de recherche du Québec - Nature et technologies (FRQNT) (#274987) and by PROTEO (Regroupement québécois de recherche sur la fonction, l'ingénierie et les applications des protéines) - FRQNT international internship (#293829) scholarships.

Author contribution statement

DS and AR conceived the study and conducted the experiment. AR, DS, CB, SR, and MPCM collected the data. AR and DS analyzed the data. AR, DS, and RS wrote the paper with input from all authors.

Competing Interests statement

The authors declare no competing interests.

References

Abbey, Darren A., Jason Funt, Mor N. Lurie-Weinberger, Dawn A. Thompson, Aviv Regev, Chad L. Myers, and Judith Berman. 2014. "YMAP: A Pipeline for Visualization of Copy Number Variation and Loss of Heterozygosity in Eukaryotic Pathogens." *Genome Medicine* 6 (11): 100.

Akache, Bassel, Sarah MacPherson, Marc-André Sylvain, and Bernard Turcotte. 2004. "Complex Interplay among Regulators of Drug Resistance Genes in Saccharomyces Cerevisiae." *The Journal of Biological Chemistry* 279 (27): 27855–60.

Ament-Velásquez, Sandra Lorena, Ciaran Gilchrist, Alexandre Rêgo, Devin P. Bendixsen, Claire Brice, Julie Michelle Grosse-Sommer, Nima Rafati, and Rike Stelkens. 2022. "The Dynamics of Adaptation to Stress from Standing Genetic Variation and de Novo Mutations." *Molecular Biology and Evolution* 39 (11). https://doi.org/10.1093/molbev/msac242.

Anderson, J. T., M. R. Wagner, C. A. Rushworth, K. V. S. K. Prasad, and T. Mitchell-Olds. 2014. "The Evolution of Quantitative Traits in Complex Environments." *Heredity* 112 (1): 4–12.

Barrett, Rowan D. H., R. Craig MacLean, and Graham Bell. 2005. "Experimental Evolution of Pseudomonas Fluorescens in Simple and Complex Environments." *The American Naturalist* 166 (4): 470–80.

Bavro, Vassiliy, Graeme L. Conn, and Christopher Davies. 2019. *Bacterial Mechanisms of Antibiotic Resistance: A Structural Perspective*. Frontiers Media SA.

Bennett, Albert F., and Richard E. Lenski. 2007. "An Experimental Test of Evolutionary Trade-Offs during Temperature Adaptation." *Proceedings of the National Academy of Sciences of the United States of America* 104 Suppl 1 (Suppl 1): 8649–54.

Bergelson, Joy, Martin Kreitman, Dmitri A. Petrov, Alvaro Sanchez, and Mikhail Tikhonov. 2021. "Functional Biology in Its Natural Context: A Search for Emergent Simplicity." *eLife* 10 (June). https://doi.org/10.7554/eLife.67646.

Bermejo, Clara, Farzad Haerizadeh, Hitomi Takanaga, Diane Chermak, and Wolf B. Frommer. 2010. "Dynamic Analysis of Cytosolic Glucose and ATP Levels in Yeast Using Optical Sensors." *Biochemical Journal* 432 (2): 399–406.

Bono, Lisa M., Leno B. Smith Jr, David W. Pfennig, and Christina L. Burch. 2017. "The Emergence of Performance Trade-Offs during Local Adaptation: Insights from Experimental Evolution." *Molecular Ecology* 26 (7): 1720–33.

Cherry, J. M., C. Adler, C. Ball, S. A. Chervitz, S. S. Dwight, E. T. Hester, Y. Jia, et al. 1998. "SGD: Saccharomyces Genome Database." *Nucleic Acids Research* 26 (1): 73–79.

Cisneros-Mayoral, Sandra, Lucía Graña-Miraglia, Deyanira Pérez-Morales, Rafael Peña-Miller, and

730 Ayari Fuentes-Hernández. 2022. "Evolutionary History and Strength of Selection Determine
731 the Rate of Antibiotic Resistance Adaptation." *Molecular Biology and Evolution* 39 (9).
732 https://doi.org/10.1093/molbev/msac185.
733 Collins, Sinéad, and Juliette de Meaux. 2009. "Adaptation to Different Rates of Environmental
734 Change in Chlamydomonas." *Evolution; International Journal of Organic Evolution* 63 (11):
735 2952–65.
736 Dhar, R., R. Sägesser, C. Weikert, J. Yuan, and A. Wagner. 2011. "Adaptation of Saccharomyces
737 Cerevisiae to Saline Stress through Laboratory Evolution." *Journal of Evolutionary Biology* 24
738 (5): 1135–53.
739 Elena, Santiago F., and Richard E. Lenski. 2003. "Evolution Experiments with Microorganisms: The
740 Dynamics and Genetic Bases of Adaptation." *Nature Reviews. Genetics* 4 (6): 457–69.
741 Ewens, W. J. 1979. *Mathematical Population Genetics*. Springer.
742 Garland, Theodore, Jr, Cynthia J. Downs, and Anthony R. Ives. 2022. "Trade-Offs (and Constraints) in
743 Organismal Biology." *Physiological and Biochemical Zoology : PBZ* 95 (1): 82–112.
744 Gordo, Isabel, Lilia Perfeito, and Ana Sousa. 2011. "Fitness Effects of Mutations in Bacteria." *Journal
745 of Molecular Microbiology and Biotechnology* 21 (1-2): 20–35.
746 Harris, Nicholas, Marcus Bachler, Vitor Costa, Mehdi Mollapour, Pedro Moradas-Ferreira, and Peter
747 W. Piper. 2005. "Overexpressed Sod1p Acts Either to Reduce or to Increase the Lifespans and
748 Stress Resistance of Yeast, Depending on Whether It Is Cu(2+)-Deficient or an Active Cu,Zn-
749 Superoxide Dismutase." *Aging Cell* 4 (1): 41–52.
750 Hendry, Andrew P., Kiyoko M. Gotanda, and Erik I. Svensson. 2017. "Human Influences on
751 Evolution, and the Ecological and Societal Consequences." *Philosophical Transactions of the
752 Royal Society of London. Series B, Biological Sciences* 372 (1712).
753 https://doi.org/10.1098/rstb.2016.0028.
754 Hickey, D. A., and T. McNeilly. 1975. "COMPETITION BETWEEN METAL TOLERANT AND NORMAL
755 PLANT POPULATIONS; A FIELD EXPERIMENT ON NORMAL SOIL." *Evolution; International
756 Journal of Organic Evolution* 29 (3): 458–64.
757 Hohmann, Stefan. 2002. "Osmotic Stress Signaling and Osmoadaptation in Yeasts." *Microbiology and
758 Molecular Biology Reviews: MMBR* 66 (2): 300–372.
759 Huang, Weini, Arne Traulsen, Benjamin Werner, Teppo Hiltunen, and Lutz Becks. 2017. "Dynamical
760 Trade-Offs Arise from Antagonistic Coevolution and Decrease Intraspecific Diversity." *Nature
761 Communications* 8 (1): 2059.
762 Hughes, Julie M., Brian K. Lohman, Gail E. Deckert, Eric P. Nichols, Matt Settles, Zaid Abdo, and Eva
763 M. Top. 2012. "The Role of Clonal Interference in the Evolutionary Dynamics of Plasmid-Host
764 Adaptation." *mBio* 3 (4): e00077–12.
765 Jani, Divyang, Sheila Lutz, Neil J. Marshall, Tamás Fischer, Alwin Köhler, Andrew M. Ellisdon, Ed
766 Hurt, and Murray Stewart. 2009. "Sus1, Cdc31, and the Sac3 CID Region Form a Conserved
767 Interaction Platform That Promotes Nuclear Pore Association and mRNA Export." *Molecular
768 Cell* 33 (6): 727–37.
769 Jarolim, Stefanie, Anita Ayer, Bethany Pillay, Allison C. Gee, Alex Phrakaysone, Gabriel G. Perrone,
770 Michael Breitenbach, and Ian W. Dawes. 2013. "Saccharomyces Cerevisiae Genes Involved in
771 Survival of Heat Shock." *G3 (Bethesda, Md.)* 3 (12): 2321–33.
772 Johnson, Milo S., Shreyas Gopalakrishnan, Juhee Goyal, Megan E. Dillingham, Christopher W.
773 Bakerlee, Parris T. Humphrey, Tanush Jagdish, et al. 2021. "Phenotypic and Molecular
774 Evolution across 10,000 Generations in Laboratory Budding Yeast Populations." *eLife* 10
775 (January). https://doi.org/10.7554/eLife.63910.
776 Jorgensen, Paul, Joy L. Nishikawa, Bobby-Joe Breitkreutz, and Mike Tyers. 2002. "Systematic
777 Identification of Pathways That Couple Cell Growth and Division in Yeast." *Science* 297 (5580):
778 395–400.
779 Karve, Shraddha, and Andreas Wagner. 2022. "Environmental Complexity Is More Important than

Mutation in Driving the Evolution of Latent Novel Traits in E. Coli." *Nature Communications* 13 (1): 5904.

Kram, Karin E., Christopher Geiger, Wazim Mohammed Ismail, Heewook Lee, Haixu Tang, Patricia L. Foster, and Steven E. Finkel. 2017. "Adaptation of to Long-Term Serial Passage in Complex Medium: Evidence of Parallel Evolution." *mSystems* 2 (2). https://doi.org/10.1128/mSystems.00192-16.

Lang, Gregory I., Daniel P. Rice, Mark J. Hickman, Erica Sodergren, George M. Weinstock, David Botstein, and Michael M. Desai. 2013. "Pervasive Genetic Hitchhiking and Clonal Interference in Forty Evolving Yeast Populations." *Nature* 500 (7464): 571–74.

Li, Yuping, Dmitri A. Petrov, and Gavin Sherlock. 2019. "Single Nucleotide Mapping of Trait Space Reveals Pareto Fronts That Constrain Adaptation." *Nature Ecology & Evolution* 3 (11): 1539–51.

MacLean, R. Craig, Alex R. Hall, Gabriel G. Perron, and Angus Buckling. 2010. "The Population Genetics of Antibiotic Resistance: Integrating Molecular Mechanisms and Treatment Contexts." *Nature Reviews. Genetics* 11 (6): 405–14.

McGee, Lindsey W., Andrew M. Sackman, Anneliese J. Morrison, Jessica Pierce, Jeremy Anisman, and Darin R. Rokyta. 2016. "Synergistic Pleiotropy Overrides the Costs of Complexity in Viral Adaptation." *Genetics* 202 (1): 285–95.

Miralles, R., P. J. Gerrish, A. Moya, and S. F. Elena. 1999. "Clonal Interference and the Evolution of RNA Viruses." *Science (New York, N.Y.)* 285 (5434): 1745–47.

Moriya, H., Y. Shimizu-Yoshida, A. Omori, S. Iwashita, M. Katoh, and A. Sakai. 2001. "Yak1p, a DYRK Family Kinase, Translocates to the Nucleus and Phosphorylates Yeast Pop2p in Response to a Glucose Signal." *Genes & Development* 15 (10): 1217–28.

Orr, H. Allen. 2005. "The Probability of Parallel Evolution." *Evolution; International Journal of Organic Evolution* 59 (1): 216–20.

Orr, James A., Pepijn Luijckx, Jean-François Arnoldi, Andrew L. Jackson, and Jeremy J. Piggott. 2022. "Rapid Evolution Generates Synergism between Multiple Stressors: Linking Theory and an Evolution Experiment." *Global Change Biology* 28 (5): 1740–52.

Orsini, Luisa, Katina I. Spanier, and Luc DE Meester. 2012. "Genomic Signature of Natural and Anthropogenic Stress in Wild Populations of the Waterflea Daphnia Magna: Validation in Space, Time and Experimental Evolution." *Molecular Ecology* 21 (9): 2160–75.

Park, Su-Chan, and Joachim Krug. 2007. "Clonal Interference in Large Populations." *Proceedings of the National Academy of Sciences of the United States of America* 104 (46): 18135–40.

Pavlicev, Mihaela, and Günter P. Wagner. 2012. "A Model of Developmental Evolution: Selection, Pleiotropy and Compensation." *Trends in Ecology & Evolution* 27 (6): 316–22.

Piper, P. W. 1995. "The Heat Shock and Ethanol Stress Responses of Yeast Exhibit Extensive Similarity and Functional Overlap." *FEMS Microbiology Letters* 134 (2-3): 121–27.

REX Consortium. 2010. "The Skill and Style to Model the Evolution of Resistance to Pesticides and Drugs." *Evolutionary Applications* 3 (4): 375–90.

Ribeiro, Gabriela Fior, Eszter Denes, Helen Heaney, and Delma S. Childers. 2022. "What 'Omics Can Tell Us about Antifungal Adaptation." *FEMS Yeast Research* 21 (8). https://doi.org/10.1093/femsyr/foab070.

Roff, D. A., and D. J. Fairbairn. 2007. "The Evolution of Trade-Offs: Where Are We?" *Journal of Evolutionary Biology* 20 (2): 433–47.

Shoval, O., H. Sheftel, G. Shinar, Y. Hart, O. Ramote, A. Mayo, E. Dekel, K. Kavanagh, and U. Alon. 2012. "Evolutionary Trade-Offs, Pareto Optimality, and the Geometry of Phenotype Space." *Science (New York, N.Y.)* 336 (6085): 1157–60.

Silva, G. S., L. Zuravski, M. M. M. F. Duarte, M. M. Machado, and L. F. S. Oliveira. 2019. "Fluconazole Induces Genotoxicity in Cultured Human Peripheral Blood Mononuclear Cells via Immunomodulation of TNF-α, IL-6, and IL-10: New Challenges for Safe Therapeutic Regimens."

Immunopharmacology and Immunotoxicology 41 (1): 123–29.
Sommer, Lea M., Helle K. Johansen, and Søren Molin. 2020. "Antibiotic Resistance in and Adaptation to Complex Dynamic Environments." *Microbial Genomics* 6 (5). https://doi.org/10.1099/mgen.0.000370.
Spampinato, Claudia, and Darío Leonardi. 2013. "Candida Infections, Causes, Targets, and Resistance Mechanisms: Traditional and Alternative Antifungal Agents." *BioMed Research International* 2013 (June):204237.
Stajic, Dragan, Lília Perfeito, and Lars E. T. Jansen. 2019. "Epigenetic Gene Silencing Alters the Mechanisms and Rate of Evolutionary Adaptation." *Nature Ecology & Evolution* 3 (3): 491–98.
Sun, Liu-Liu, Hao Li, Tian-Hua Yan, Yong-Bing Cao, Yuan-Ying Jiang, and Feng Yang. 2023. "Aneuploidy Enables Cross-Tolerance to Unrelated Antifungal Drugs in." *Frontiers in Microbiology* 14 (April):1137083.
Vandenkoornhuyse, Philippe, Alexis Dufresne, Achim Quaiser, Gwenola Gouesbet, Françoise Binet, André-Jean Francez, Stéphane Mahé, Myriam Bormans, Yvan Lagadeuc, and Ivan Couée. 2010. "Integration of Molecular Functions at the Ecosystemic Level: Breakthroughs and Future Goals of Environmental Genomics and Post-Genomics." *Ecology Letters* 13 (6): 776–91.
Venkataram, Sandeep, and Sergey Kryazhimskiy. 2023. "Evolutionary Repeatability of Emergent Properties of Ecological Communities." *Philosophical Transactions of the Royal Society of London. Series B, Biological Sciences* 378 (1877): 20220047.
Vincent, Benjamin Matteson, Alex Kelvin Lancaster, Ruth Scherz-Shouval, Luke Whitesell, and Susan Lindquist. 2013. "Fitness Trade-Offs Restrict the Evolution of Resistance to Amphotericin B." *PLoS Biology* 11 (10): e1001692.
Waldvogel, Ann-Marie, Barbara Feldmeyer, Gregor Rolshausen, Moises Exposito-Alonso, Christian Rellstab, Robert Kofler, Thomas Mock, et al. 2020. "Evolutionary Genomics Can Improve Prediction of Species' Responses to Climate Change." *Evolution Letters* 4 (1): 4–18.
Wang, Wen-Yao, Hong-Qing Cai, Si-Yuan Qu, Wei-Hao Lin, Cheng-Cheng Liang, Hao Liu, Ze-Xiong Xie, and Ying-Jin Yuan. 2022. "Genomic Variation-Mediating Fluconazole Resistance in Yeast." *Biomolecules* 12 (6). https://doi.org/10.3390/biom12060845.
Watanabe, Machika, Daisuke Watanabe, Satoru Nogami, Shinichi Morishita, and Yoshikazu Ohya. 2009. "Comprehensive and Quantitative Analysis of Yeast Deletion Mutants Defective in Apical and Isotropic Bud Growth." *Current Genetics* 55 (4): 365–80.
Wiser, Michael J., Noah Ribeck, and Richard E. Lenski. 2013. "Long-Term Dynamics of Adaptation in Asexual Populations." *Science* 342 (6164): 1364–67.
Yüzbaşioğlu, Deniz, Fatma Unal, Serkan Yilmaz, Hüseyin Aksoy, and Mustafa Celik. 2008. "Genotoxicity Testing of Fluconazole in Vivo and in Vitro." *Mutation Research* 649 (1-2): 155–60.
Zelnik, Yuval R., Nuria Galiana, Matthieu Barbier, Michel Loreau, Eric Galbraith, and Jean-François Arnoldi. 2024. "How Collectively Integrated Are Ecological Communities?" *Ecology Letters* 27 (1): e14358.
Zhang, Xiao, Mark Blaxter, Jonathan M. D. Wood, Alan Tracey, Shane McCarthy, Peter Thorpe, Jack G. Rayner, et al. 2024. "Temporal Genomics in Hawaiian Crickets Reveals Compensatory Intragenomic Coadaptation during Adaptive Evolution." *Nature Communications* 15 (1): 5001.

Supplementary Materials

Treatment	Population	Compensation	Mutations gained	Mutations lost

N	NASH1	S_{T7}=-0.21 S_{T15}=0.12	SKY1 PRC1 tE(UUC)Q* BI2 BI3	CSG2
	NSA3	S_{T7}=-0.04 S_{T15}=0.22	RIM15 MYO5	FCY2 INP1*
	NSA4	S_{T7}=-0.01 S_{T15}=0.24	GPI17 RIM15	TEC1 ERV14* TIR4
A	SAH3	S_{T7}=-0.43 S_{T15}=0.44	ITC1 PUF3 PSR1	
	SAH4	S_{T7}=-0.37 S_{T15}=0.46	SOD1 ROX1	
	NSA1	S_{T7}=-0.19 S_{T15}=0.46	RIM15 PDR1	BIL1*
S	NSH2	S_{T7}=-0.29 S_{T15}=0.19	OKP1 THP2 YIL055C* IRA2 PUF3	AUR1
	NSH1	S_{T7}=-0.24 S_{T15}=0.12	SAC3 MCM1	
	NASH1	S_{T7}=-0.45 S_{T15}=-0.13	SKY1 PRC1 tE(UUC)Q* BI2 BI3	CSG2
H	NSH2	S_{T7}=-0.23 S_{T15}=0.1	OKP1 THP2 YIL055C* IRA2 PUF3	AUR1
	NSH3	S_{T7}=-0.28 S_{T15}=-0.05	SUB2 SAC3 EEB1	
	NASH1	S_{T7}=-0.38 S_{T15}=-0.14	SKY1 PRC1 tE(UUC)Q* BI2 BI3	CSG2

873 Supplementary Table 1. Gene mutations gained or lost during compensatory evolution
874 (from T7 to T15). The three lines with the greatest compensatory changes (where S_{T7} <0)
875 in fitness are shown per individual stressor. Gains and losses of gene mutations are shown
876 in green and red, respectively. Asterisks designate upstream gene mutations not found in
877 the protein coding region.
878

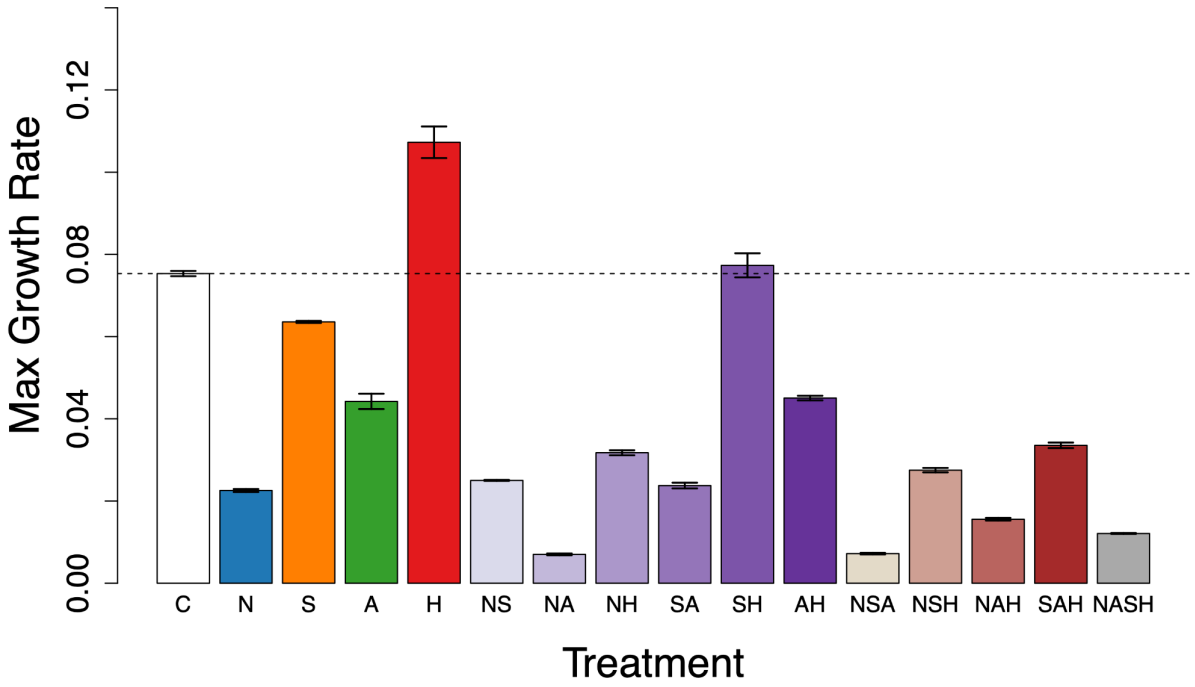

Supplementary Figure 1. The stressor effect of each environment in the ancestor is measured as the difference in maximum growth rate in a selective environment relative to benign YPD medium. The mean estimate is given and error bars represent the standard error.

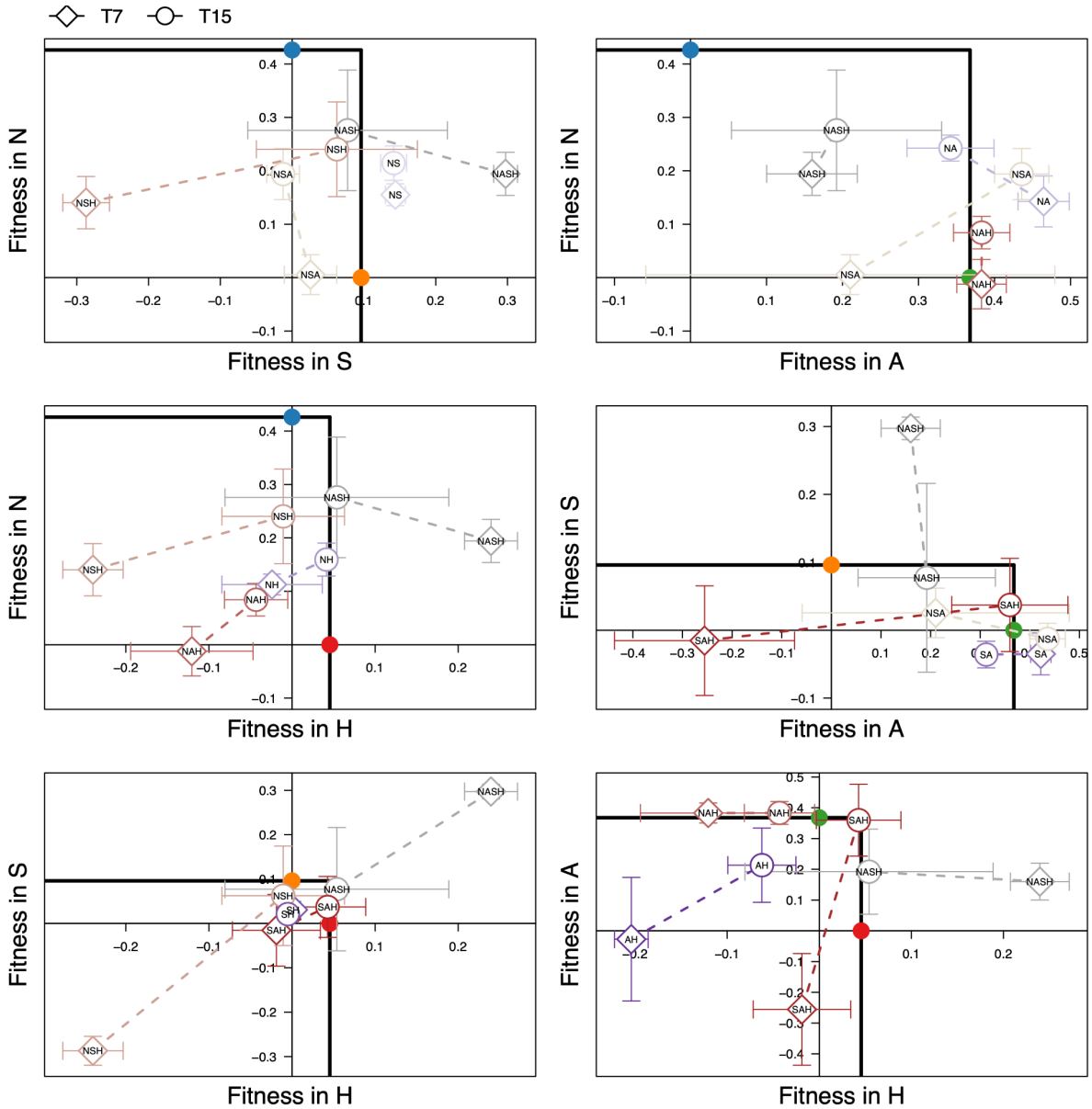

Supplementary Figure 2. Trade-off trajectories of populations adapted to complex environments visualized for every two-way combination of individual environmental components. For each panel, the means of each line evolved in those two environmental components are shown as diamonds or circles for T7 and T15, respectively. Standard errors for selection coefficients are shown as bars for the respective axes (see Figure S1 for individual treatments). Maximum observed fitness of single environment specialists is shown as colored points projected along the respective axes. The solid black lines represent the space in which complex environments are expected to fall (i.e. less adapted in individual environments than either individual-environment specialist).

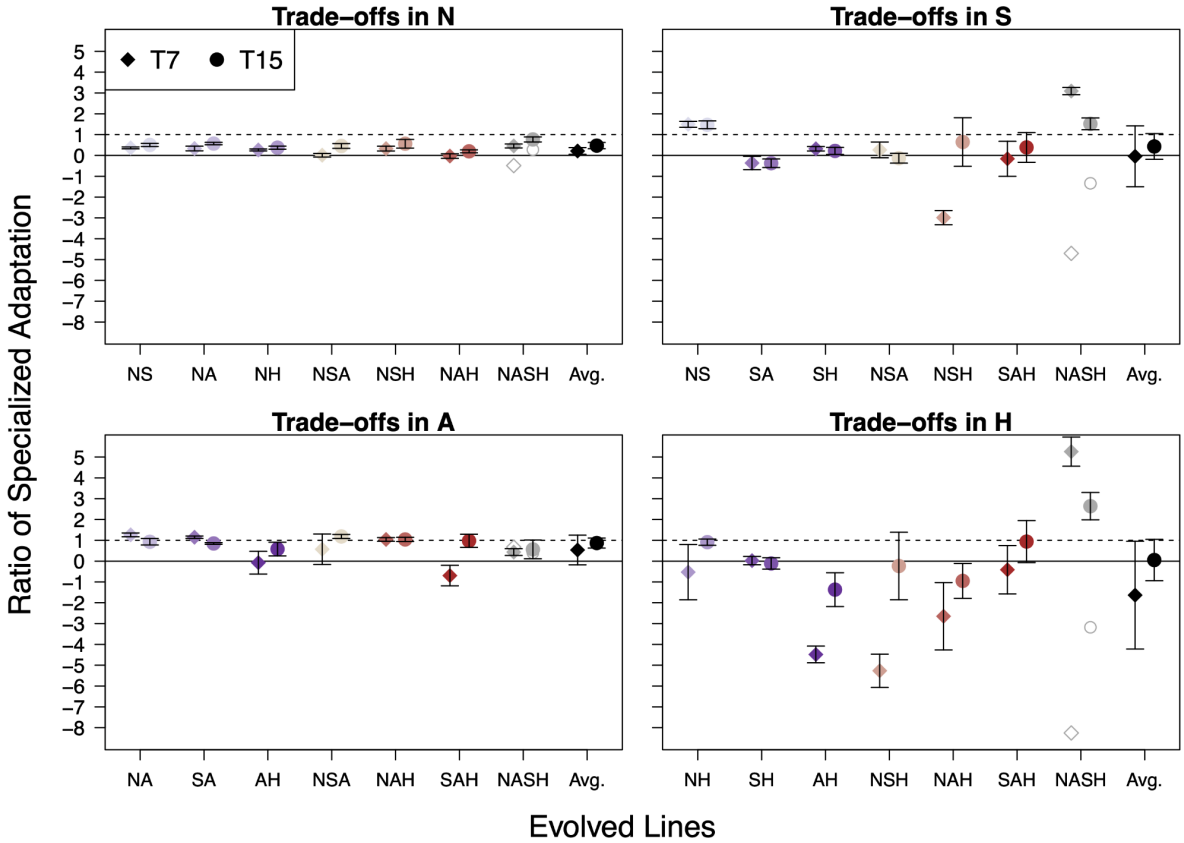

Supplementary Figure 3. Trade-offs in each individual component of complex environment treatments. Adaptation to the individual environment by the 1D specialist are shown as projections along the respective axes. Within the lower-left of the black dotted lines represents the space in which complex environments are expected to fall (i.e. less adapted in single-environments than either 1D specialist). Means are shown as diamonds or circles for T7 and T15, respectively. Standard deviations for selection coefficients are shown as bars for the respective axes.

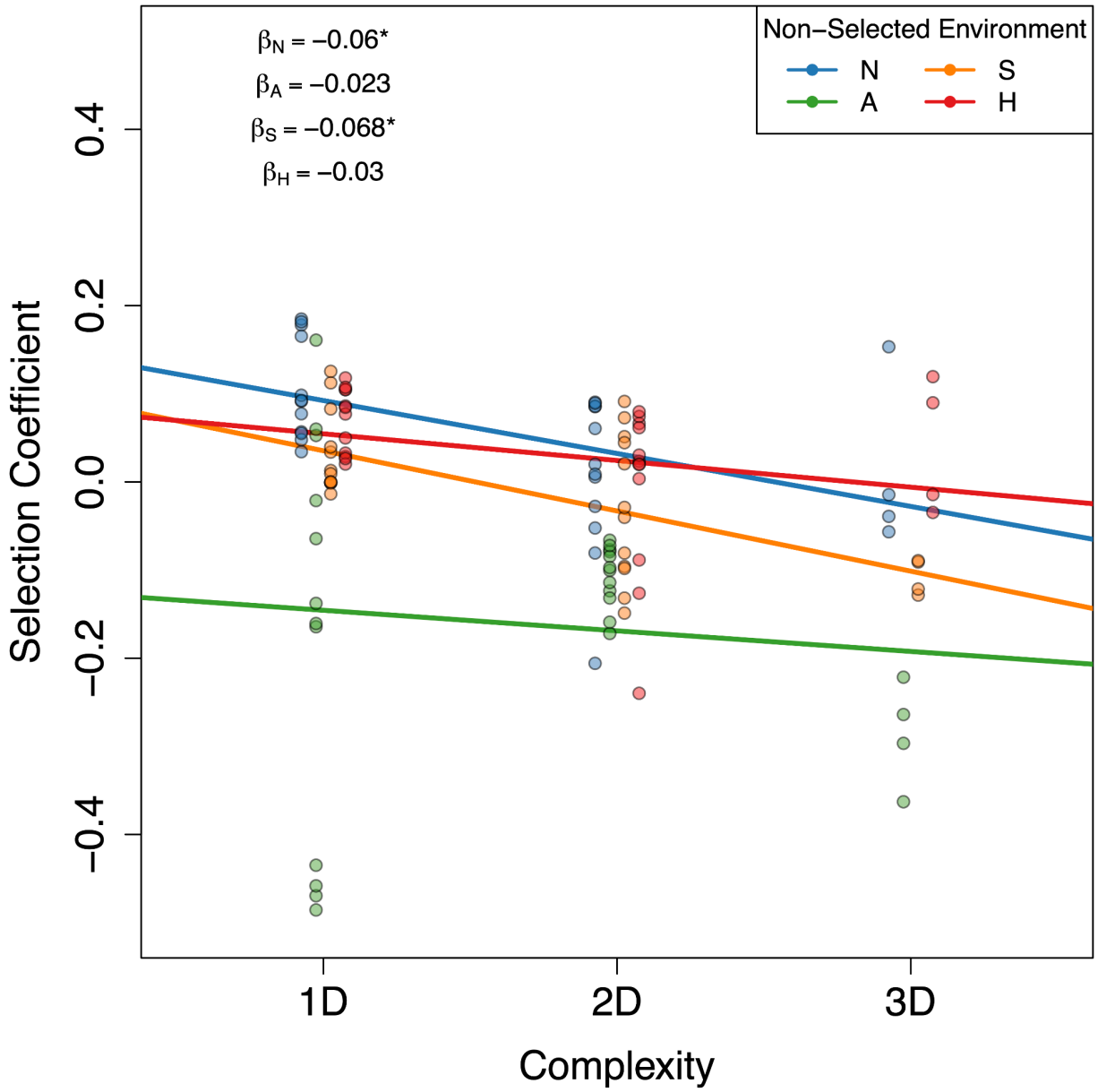

Supplementary Figure 4. Fitness declines with environmental complexity in non-selected environments. Selection coefficients (i.e., relative fitness to the ancestor) are shown for evolved lines at T15 in test environments they were not exposed to during experimental evolution. The slope of the linear regression between fitness and complexity are shown for each non-selected environment, with significant slopes designated by an asterisk.

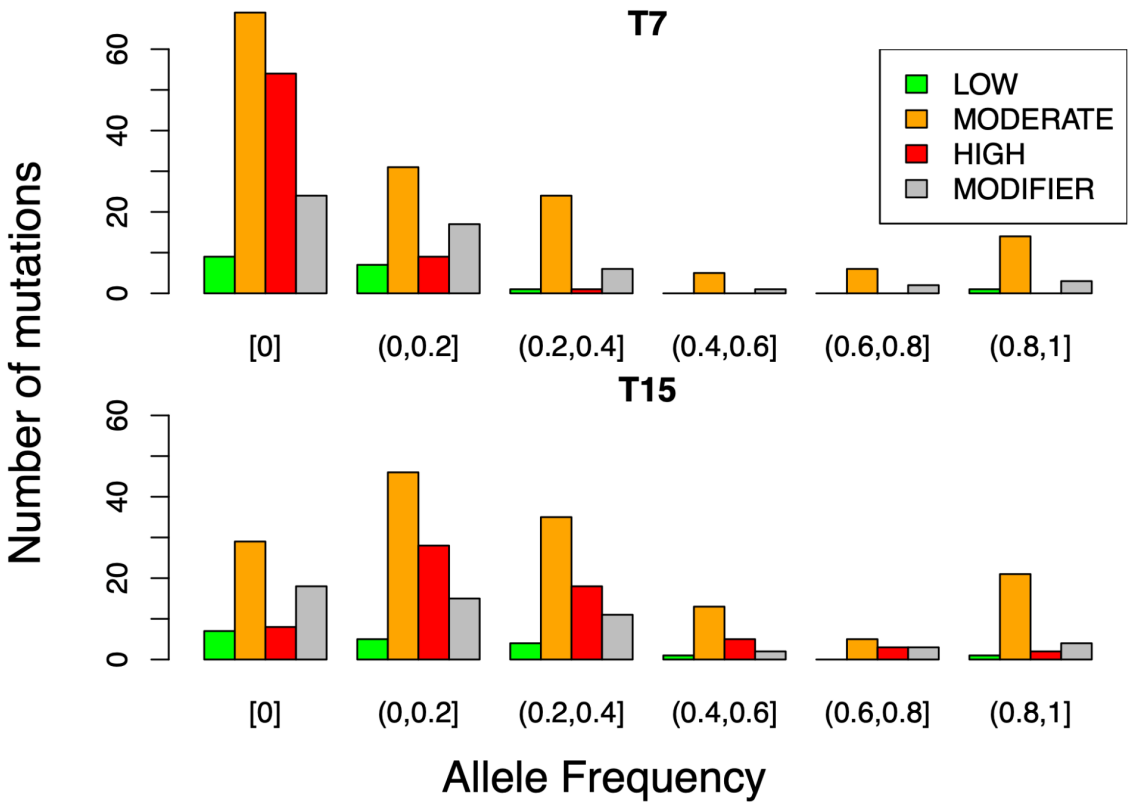

Supplementary Figure 5. The number of types of mutations (SNPs and INDELs) across all evolved populations categorized by snpEff, binned by allele frequency. Mutations at AF=0 in T7 did not yet arise in any of the populations, and mutations at AF=0 in T15 are those that previously existed at T7 but were subsequently eliminated.

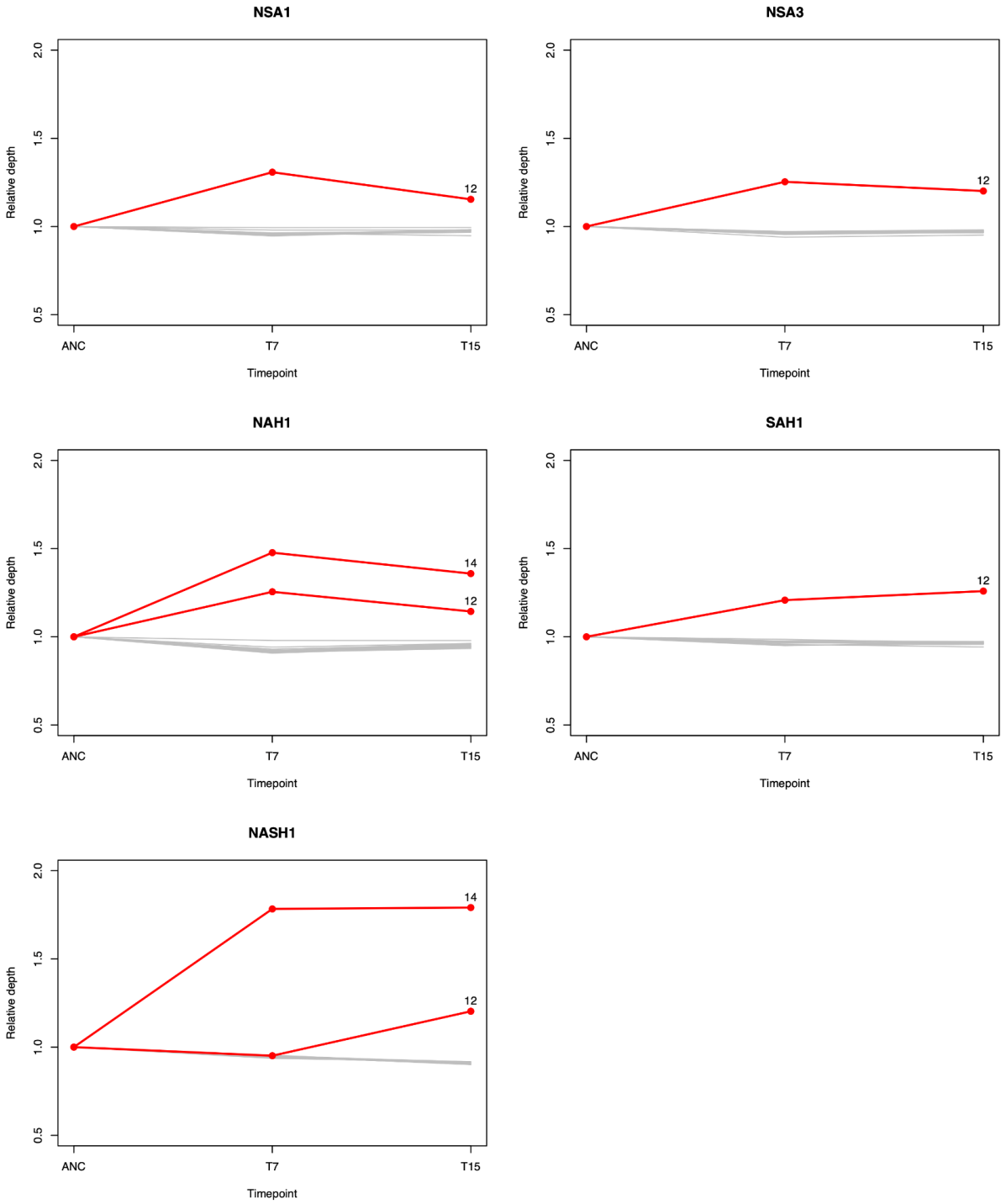

Supplementary Figure 6. Aneuploidies identified in five populations. Plotted are the mean relative depths of each chromosome standardized to the ancestral population. In red are chromosomes which deviate from the ancestor relative depth by more than 20%. Putative aneuploidies are labeled with chromosome number.

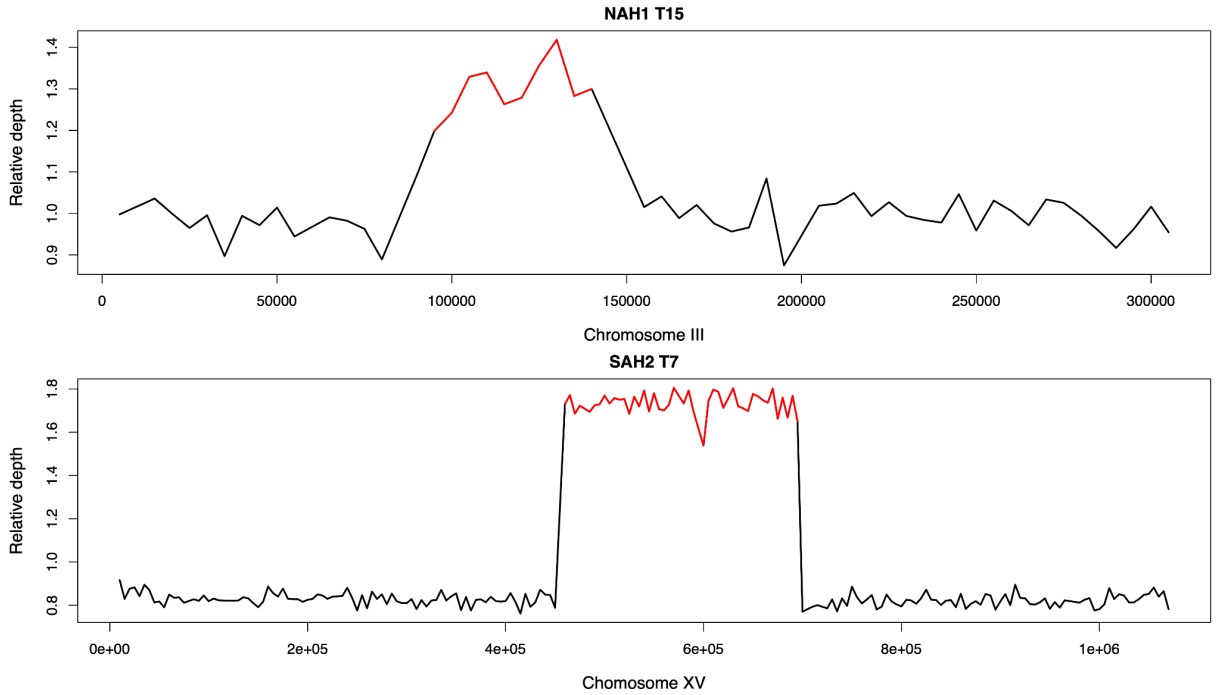

Supplementary Figure 7. Copy number variants in two populations. Plotted are the mean relative depth across the genome in 5kb non-overlapping windows. In red are segments which deviate from the ancestor relative depth by more than 20%.

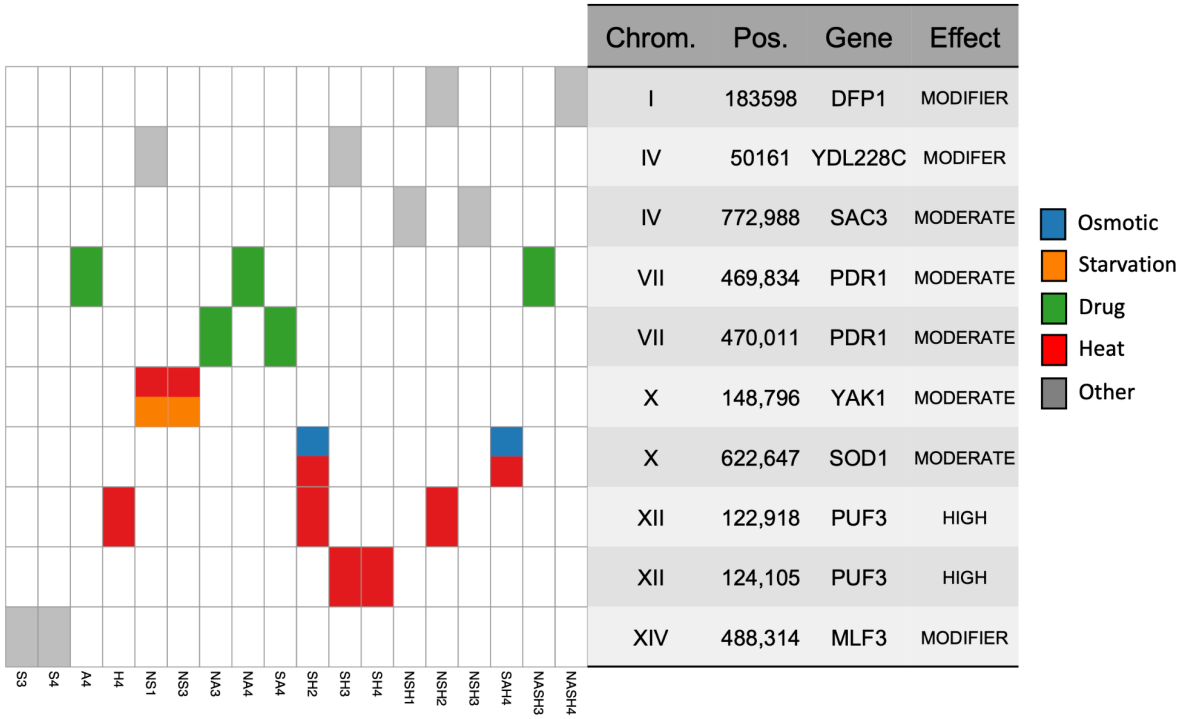

Chrom.	Pos.	Gene	Effect
I	183598	DFP1	MODIFIER
IV	50161	YDL228C	MODIFER
IV	772,988	SAC3	MODERATE
VII	469,834	PDR1	MODERATE
VII	470,011	PDR1	MODERATE
X	148,796	YAK1	MODERATE
X	622,647	SOD1	MODERATE
XII	122,918	PUF3	HIGH
XII	124,105	PUF3	HIGH
XIV	488,314	MLF3	MODIFIER

Supplementary Figure 8. Recurrent mutations at specific SNPs across independent evolved populations. Shared mutations are colored by the parental GO category, white is no shared mutation. The table presents the chromosome, position, gene name, and predicted effect

933 given by SnpEff for each mutation. Populations which do not contain a recurrent mutation
934 are not shown.
935

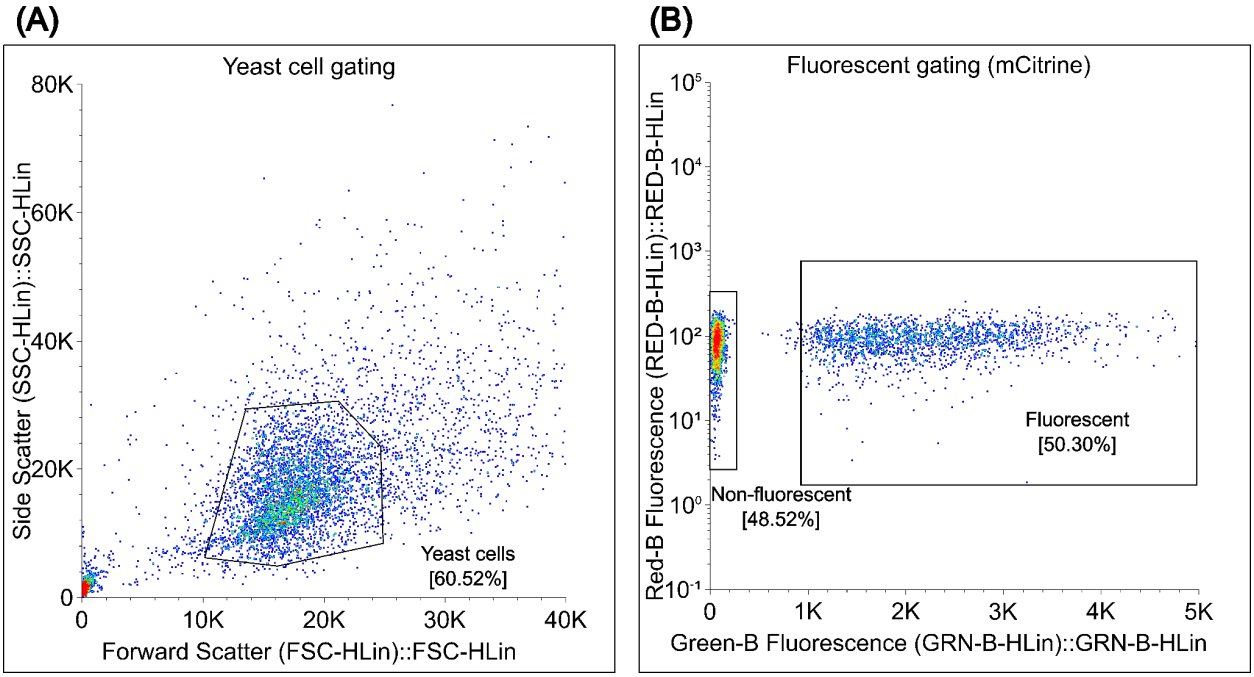

936
937 Supplementary Figure 9. Example of gating strategy for flow cytometry. Points indicate
938 individual events, and are colored by density (blue, low density; red, high density). A) Yeast
939 cells were identified using a FSC gate between 10000 to 25000, and a SSC gate between
940 6000 to 30000. B) The proportions of fluorescent ancestral yeast to non-fluorescent
941 ancestral or evolved lines were then discriminated using a blue 488nm laser with emission
942 intensity (GRN-B-Hlin) greater than 1000 indicating the fluorescent ancestral cell. Note
943 that the fluorescent ancestor and tested line appear at approximately a 1:1 ratio at 0 h of
944 flow cytometry for this example.